Lentivector Iterations and Pre-Clinical Scale-Up/Toxicity Testing: Targeting Mobilized CD34+ Cells for Correction of Fabry Disease

Molecular Therapy
Methods & Clinical Development
Original Article

Lentivector Iterations and Pre-Clinical Scale-Up/Toxicity Testing: Targeting Mobilized CD34$^+$ Cells for Correction of Fabry Disease

Ju Huang,[1] Aneal Khan,[2] Bryan C. Au,[1] Dwayne L. Barber,[1,3,4] Lucía López-Vásquez,[1,5] Nicole L. Prokopishyn,[6] Michel Boutin,[7] Michael Rothe,[8] Jack W. Rip,[9] Mona Abaoui,[7] Murtaza S. Nagree,[1,4] Shaalee Dworski,[1,5] Axel Schambach,[8,10] Armand Keating,[1] Michael L. West,[11] John Klassen,[12] Patricia V. Turner,[13] Sandra Sirrs,[14] C. Anthony Rupar,[9] Christiane Auray-Blais,[7] Ronan Foley,[15] and Jeffrey A. Medin[1,4,5,16,17]

[1]University Health Network, Toronto, ON M5G 1L7, Canada; [2]Department of Medical Genetics, Alberta Children's Hospital Research Institute, Cumming School of Medicine, University of Calgary, Calgary, AB T2N 4N1, Canada; [3]Department of Laboratory Medicine and Pathobiology, University of Toronto, Toronto, ON M5S 1A8, Canada; [4]Department of Medical Biophysics, University of Toronto, Toronto, ON M5G 1L7, Canada; [5]Institute of Medical Science, University of Toronto, Toronto, ON M5S 1A8, Canada; [6]Department of Pathology and Laboratory Medicine, University of Calgary and Cellular Therapy Laboratory, Calgary Lab Services, Calgary, AB T2N 1N4, Canada; [7]Division of Medical Genetics, Department of Pediatrics, Université de Sherbrooke, Sherbrooke, QC J1K 2R1, Canada; [8]Institute of Experimental Hematology, Hannover Medical School, 30625 Hannover, Germany; [9]Department of Pathology and Laboratory Medicine, Western University, London, ON N6A 5C1, Canada; [10]Division of Hematology/Oncology, Boston Children's Hospital, Harvard Medical School, Boston, MA 02115, USA; [11]Division of Nephrology, Department of Medicine, Dalhousie University, Halifax, NS B3H 1V8, Canada; [12]Department of Hematology, University of Calgary, Foothills Hospital, Calgary, AB T2N 2T9, Canada; [13]Department of Pathobiology, University of Guelph, Guelph, ON N1G 2W1, Canada; [14]Division of Endocrinology, Department of Medicine, University of British Columbia, Vancouver, BC V5Z 1M9, Canada; [15]Juravinski Hospital and Cancer Centre, Hamilton, ON L8V 5C2, Canada; [16]Medical College of Wisconsin, Milwaukee, WI 53226, USA

Fabry disease is a rare lysosomal storage disorder (LSD). We designed multiple recombinant lentivirus vectors (LVs) and tested their ability to engineer expression of human α-galactosidase A (α-gal A) in transduced Fabry patient CD34$^+$ hematopoietic cells. We further investigated the safety and efficacy of a clinically directed vector, LV/AGA, in both ex vivo cell culture studies and animal models. Fabry mice transplanted with LV/AGA-transduced hematopoietic cells demonstrated α-gal A activity increases and lipid reductions in multiple tissues at 6 months after transplantation. Next we found that LV/AGA-transduced Fabry patient CD34$^+$ hematopoietic cells produced even higher levels of α-gal A activity than normal CD34$^+$ hematopoietic cells. We successfully transduced Fabry patient CD34$^+$ hematopoietic cells with "near-clinical grade" LV/AGA in small-scale cultures and then validated a clinically directed scale-up transduction process in a GMP-compliant cell processing facility. LV-transduced Fabry patient CD34$^+$ hematopoietic cells were subsequently infused into NOD/SCID/Fabry (NSF) mice; α-gal A activity corrections and lipid reductions were observed in several tissues 12 weeks after the xenotransplantation. Additional toxicology studies employing NSF mice xenotransplanted with the therapeutic cell product demonstrated minimal untoward effects. These data supported our successful clinical trial application (CTA) to Health Canada and opening of a "first-in-the-world" gene therapy trial for Fabry disease.

INTRODUCTION

Fabry disease (OMIM no. 301500) occurs because of a deficiency of α-galactosidase A (α-gal A; EC 3.2.1.22) activity.[1] Glycosphingolipids such as globotriaosylceramide (Gb_3) accumulate in Fabry disease. This build-up ultimately leads to end-organ damage in the kidneys, heart, and brain.[2] The *GLA* gene that encodes for α-gal A is found on the X chromosome; both men and heterozygous women have clinical manifestations of Fabry disease. Life expectancy with Fabry disease is decreased in males to 58.2 years and in females to 75.4 years.[3] The prevalence of males with Fabry disease ranges from 1:17,000 to 1:117,000 in the Caucasian population.[4,5] Recent newborn screening studies have, however, indicated a much higher incidence of this disorder because patients with later onset and milder forms of Fabry disease are found even more commonly than expected, suggesting that they are possibly underdiagnosed.[6–13]

Enzyme replacement therapy (ERT) is the only Food and Drug Administration (FDA)-approved treatment for Fabry disease to date. Last year, oral pharmacological chaperone therapy was

Received 20 January 2017; accepted 8 May 2017;
http://dx.doi.org/10.1016/j.omtm.2017.05.003.

[17]Present address: Medical College of Wisconsin, 8701 Watertown Plank Road, CRI: C4540, Milwaukee, WI 53226, USA.

Correspondence: Jeffrey A. Medin, Medical College of Wisconsin, 8701 Watertown Plank Road, CRI: C4540, Milwaukee, WI 53226, USA.
E-mail: jmedin@mcw.edu

approved by the European Commission to treat Fabry patients in the European Union (EU) with an amenable mutation of α-gal A.[14] Our group and others have been developing gene therapy for this disorder for nearly 20 years.[15–23] We previously showed that "metabolic cooperativity" or "cross-correction" occurs for Fabry disease. This means that genetically augmented cells are not only corrected enzymatically themselves but also facilitate extracellular secretion of α-gal A that can be taken up and used functionally by unmodified bystander cells.[17,20] Our previous studies in Fabry mice showed that metabolic cooperativity is manifested in multiple organs over long periods of time (even in secondary recipient animals) following genetic correction of primitive hematopoietic cells.[24] Therefore, targeting $CD34^+$ hematopoietic stem cells (HSCs)/progenitor cells for gene augmentation is a promising strategy to achieve long-term enzyme correction in the blood and organs in patients with Fabry disease. We have also developed the non-obese diabetic (NOD)/severe combined immunodeficiency (SCID)/Fabry (NSF) mouse model for in vivo efficacy and toxicity studies with our lentivirus (LV) vector-transduced human cell product.[15]

Here we constructed multiple novel recombinant LV vectors in a sequential fashion that engineered expression of α-gal A and compared their functionality following ex vivo transduction of mobilized Fabry patient $CD34^+$ hematopoietic cells. This was done in preparation for a clinical trial application (CTA) to Health Canada. Two early-version vectors that contained a "cell-fate control" or "suicide" element and/or a cell surface marker sequence only yielded 10%–30% α-gal A activity of that seen in control normal cells. A later-generation construct (LV/AGA) consisting of only the human codon-optimized *GLA* cDNA with a canonical Kozak sequence produced higher-than-normal levels of α-gal A in transduced Fabry patient $CD34^+$ hematopoietic cells. This vector was used as the "clinically directed reagent" going forward for all our preclinical efficacy and safety studies. This vector was also tested in long-term Fabry mouse-to-Fabry mouse experiments; no untoward effects were seen, and enzyme correction/lipid reduction were observed.

Next we developed a translatable protocol to successfully transduce Fabry patient $CD34^+$ hematopoietic cells ex vivo with a "near-clinical-grade" preparation of LV/AGA. The vector was made by the Indiana University Vector Production Facility (IUVPF). Transduced cells were subsequently infused into NSF mice. A significant increase in α-gal A activity was observed in the plasma, bone marrow, spleens, and livers of transplanted NSF mice. Mass spectrometry (MS) results showed a reduction of total Gb3 levels in spleens and livers. Following this, we performed an independent toxicology study on xenotransplanted NSF mice and observed minimal in vivo perturbations from the therapeutic cell product. Finally, we validated scale-up transduction experiments in a cell processing facility at the University Health Network (UHN) under good manufacturing practices (GMP) conditions to meet CTA requirements. Our preclinical data in animals and validated scale-up LV-transduction processes, utilizing $CD34^+$ hematopoietic cells, provided essential evidence to support opening of a phase I gene therapy trial to treat patients with Fabry disease.

RESULTS

Ex Vivo Transduction of $CD34^+$ Hematopoietic Cells with Multiple LV Iterations and Development of a Clinically Directed Product

We had previously constructed an LV transfer vector, pDY.ΔLNGFR/TMPK.IRES.CO.α-gal A, which is a bicistronic vector comprised of the cDNA of a cell-fate control element, ΔLNGFR/modified human thymidylate kinase (TMPK) as the first transgene, followed by an internal ribosome entry site (IRES), and then the cDNA of the human *GLA* gene encoding normal α-gal A enzyme—all under the control of the mammalian elongation factor 1 α (EF-1α) promoter.[16] The cDNA of the ΔLNGFR/TMPK component encodes a fusion form of the truncated human low-affinity nerve growth factor receptor (ΔLNGFR) combined with mutant TMPK. ΔLNGFR serves as a cell surface protein marker, and the mutant TMPK induces cell death by downstream-phosphorylating the prodrug 3′-azido-3′-deoxythymidine (AZT) to AZT-DP and, thus, is a "suicide gene" when transduced cells need to be eliminated for any reason.[15] Furthermore, the cDNAs of both the ΔLNGFR/TMPK element and the human *GLA* sequence were codon-optimized to enhance expression in human cells. The LV produced from this transfer vector (LV/FAB) has been previously shown by us to engineer good α-gal A expression in Fabry patient B cells and in supernatants from transduced normal $CD34^+$ hematopoietic cells. Such transductions also rendered cells sensitive to AZT treatment.[16]

Near-clinical-grade LV/FAB was produced under contract with the IUVPF in a GMP facility. The near-clinical-grade vector was manufactured in the same facility and follows the same procedures as the clinical-grade vector that is being used for our phase I gene therapy trial in Fabry patients (https://clinicaltrials.gov, NCT02800070). Processing is the same, except that the latter version has more extensive quality control/quality assurance testing and documentation.

We first examined the transduction fidelity and functionality of LV/FAB in ex vivo-cultured mobilized peripheral blood $CD34^+$ hematopoietic cells collected from a classically affected male Fabry patient (no. 14-159) following our protocol as described in Materials and Methods. Normal $CD34^+$ hematopoietic cells from healthy donors were included in parallel as a positive control. Secreted (culture supernatant) and intracellular (cell lysate) α-gal A activity was measured. We found an efficient transduction frequency of 65%–85% in Fabry patient $CD34^+$ hematopoietic cells by staining for truncated LNGFR expression followed by flow cytometry analyses (Figure S1A). Mock-transduced Fabry patient $CD34^+$ hematopoietic cells (MOI = 0) showed minimal α-gal A activity in cell lysates and negligible secreted activity in the supernatant (Figures S1B and S1C). Unfortunately, LV/FAB-transduced Fabry patient $CD34^+$ hematopoietic cells only demonstrated a small increase in α-gal A activity, to ~10% of the level seen in normal $CD34^+$ cells, at an MOI of 18. Even with LV/FAB at an MOI of 80, the level of α-gal A activity in transduced Fabry $CD34^+$ hematopoietic cells only reached ~30% of that seen in normal $CD34^+$ hematopoietic cells (Figure S1C). At this point, a decision was made that this vector construct did not warrant progression into the clinic.

We next examined the DNA sequence of the transfer vector used above and found that the sequence surrounding the start codon of the *GLA* cDNA (CCCACC) was not the canonical eukaryotic Kozak consensus sequence (GCC(AorG)CC), which has a conserved G at the −6-bp position from the start codon.[25] Therefore, we adjusted the sequence surrounding the start codon in the LV/FAB transfer vector and made a new LV preparation in our laboratory. This new research-grade LV/FAB-2 performed slightly better in $CD34^+$ hematopoietic cells, enabling transduced Fabry patient cells to secrete a similar or higher level of α-gal A enzyme (at MOI 18 and 80) than normal cells (Figure S1B). However, intracellular α-gal A activity from LV/FAB-2-transduced Fabry patient $CD34^+$ hematopoietic cells was still only 10% of that observed from normal cells (Figure S1C).

In parallel with the preceding studies, we compared another vector, LV/α-gal A.IRES.hCD25, which had been constructed and used previously in our lab.[15,26] This vector consisted of an EF-1α promoter-driven cDNA encoding wild-type human α-gal A followed by an IRES.hCD25 sequence.[26] We found that Fabry $CD34^+$ hematopoietic cells transduced with this vector produced higher levels of α-gal A than LV/FAB and LV/FAB-2 in both medium supernatant and cell lysates (Figures S1B and S1C). Even though the secreted level of α-gal A activity from LV/α-gal A.IRES.hCD25-tranduced Fabry patient $CD34^+$ hematopoietic cells reached 1.2- to 4.2-fold higher than that from normal cells, the intracellular level of α-gal A activity was still only 17%–31% of normal cells depending on the MOI used (Figures S1B and S1C). These results suggest that the bicistronic vector orientation (specifically the inclusion of an IRES element) may affect the efficiency of downstream α-gal A translation in transduced $CD34^+$ hematopoietic cells.

To develop a more efficient LV that can produce higher levels of α-gal A in transduced target $CD34^+$ hematopoietic cells and fulfill our clinical directive, we constructed another new transfer vector, pDY.CO.α-gal A (LV/AGA), consisting of a codon-optimized cDNA of human *GLA* under the control of the EF-1α promoter (Figure 1A). This vector also maintains the optimized Kozak sequence around the initiation codon. A LV using this simplest transfer vector (LV/AGA) was prepared in our laboratory (research-grade) and tested for transduction of Fabry $CD34^+$ hematopoietic cells (patient no. 14-159). As shown in Figures S1B and S1C, LV/AGA-transduced Fabry cells showed significantly increased α-gal A activity in both the supernatant (4.6-fold over normal cells) and the cell lysates. In fact, α-gal A activity levels in lysates from cell pellets that had been infected at an MOI of 10 were even higher than those observed in normal cells. Transduced cells showed lower α-gal A activity at an MOI of 50 than what was observed at an MOI of 10, suggesting some sort of inhibition or a toxic effect on cells at higher MOIs using this research-grade vector preparation. We repeated the transduction experiment two more times at an MOI of 10 on the same patient cells and obtained similar results (Figure 1B). Therefore, we decided to use LV/AGA as the vector for the rest of the pre-clinical studies and for a subsequent phase I gene therapy trial treating Fabry patients (which has now been approved by Health Canada; see https://clinicaltrials.gov).

We also investigated the optimal MOI for transduction with the clinically directed vector. Fabry patient $CD34^+$ hematopoietic cells were transduced with research-grade LV/AGA at MOIs of 0, 5, 10, 15, and 20. α-Gal A activity in lysates from transduced target cells increased with MOIs up to 10, and then the enzyme activity again reduced at MOIs of 15 and 20 (Figure 1D); hence, we decided to use an MOI of 10 for transductions in the rest of the study to achieve maximal efficacy.

Pre-clinical Validations of LV/AGA In Vitro in Fabry Patient $CD34^+$ Hematopoietic Cells

Near-clinical-grade LV/AGA was subsequently produced by IUVPF as described in Materials and Methods. This product was tested by transduction of mobilized $CD34^+$ hematopoietic cells from a healthy donor as well as from two Fabry patients (nos. 14-159 and 15-220). The results are shown in Figures 1C and 1E, respectively. Consistent with the results from research-grade LV/AGA, both secreted and intracellular α-gal A activities were minimal in mock-transduced Fabry cells but substantially elevated in LV/AGA-transduced Fabry cells to a level 20% higher than mock-transduced normal cells (Figures 1C and 1E). Furthermore, α-gal A activity from LV/AGA-transduced normal cells was also more than 2-fold higher than the α-gal A activity from mock-transduced normal cells (Figure 1C).

To determine the core near-clinical-grade LV/AGA transduction efficiency of the $CD34^+$ hematopoietic cells, we examined average viral copy number (VCN) per genome by qPCR along with the percentage of LV-positive cells by colony-forming cell (CFC) assays (Table 1). An average of 0.25, 0.43, and 0.33 VCNs/genome were obtained from transduced normal, transduced Fabry patient no. 14-159, and transduced Fabry patient no. 15-220 cells, respectively. As negative controls, 0 VCN/genome was obtained from all mock-transduced cells. To evaluate the transduction frequency of $CD34^+$ stem/progenitor cells using our protocol, we performed CFC assays by growing LV-transduced cells in methylcellulose and testing for the percentage of LV-integrated cell-derived colonies as described in Materials and Methods. Forty-six percent (26 of 56 colonies) and 20% (22 of 111 colonies) of LV/AGA-transduced cells corresponding to Fabry patient no. 14-159 and Fabry patient no. 150-220 samples, respectively, were positive for the woodchuck hepatitis virus post-transcriptional regulatory element (WPRE) (LV-derived), consistent with the aforementioned VCN results.

These data show that, at an MOI of 10, 20%–50% of primitive hematopoietic cells had stable LV/AGA integration, and those transduced cells expressed α-gal A activities to the level of that observed in extracts from normal human $CD34^+$ hematopoietic cells.

Safety and Efficacy of Clinically Directed LV/AGA in Fabry Mouse-to-Fabry Mouse Experiments

To investigate the long-term efficacy of LV/AGA and our cell product and to ensure that there were no untoward effects in vivo from this recombinant vector, we carried out mouse-to-mouse bone marrow

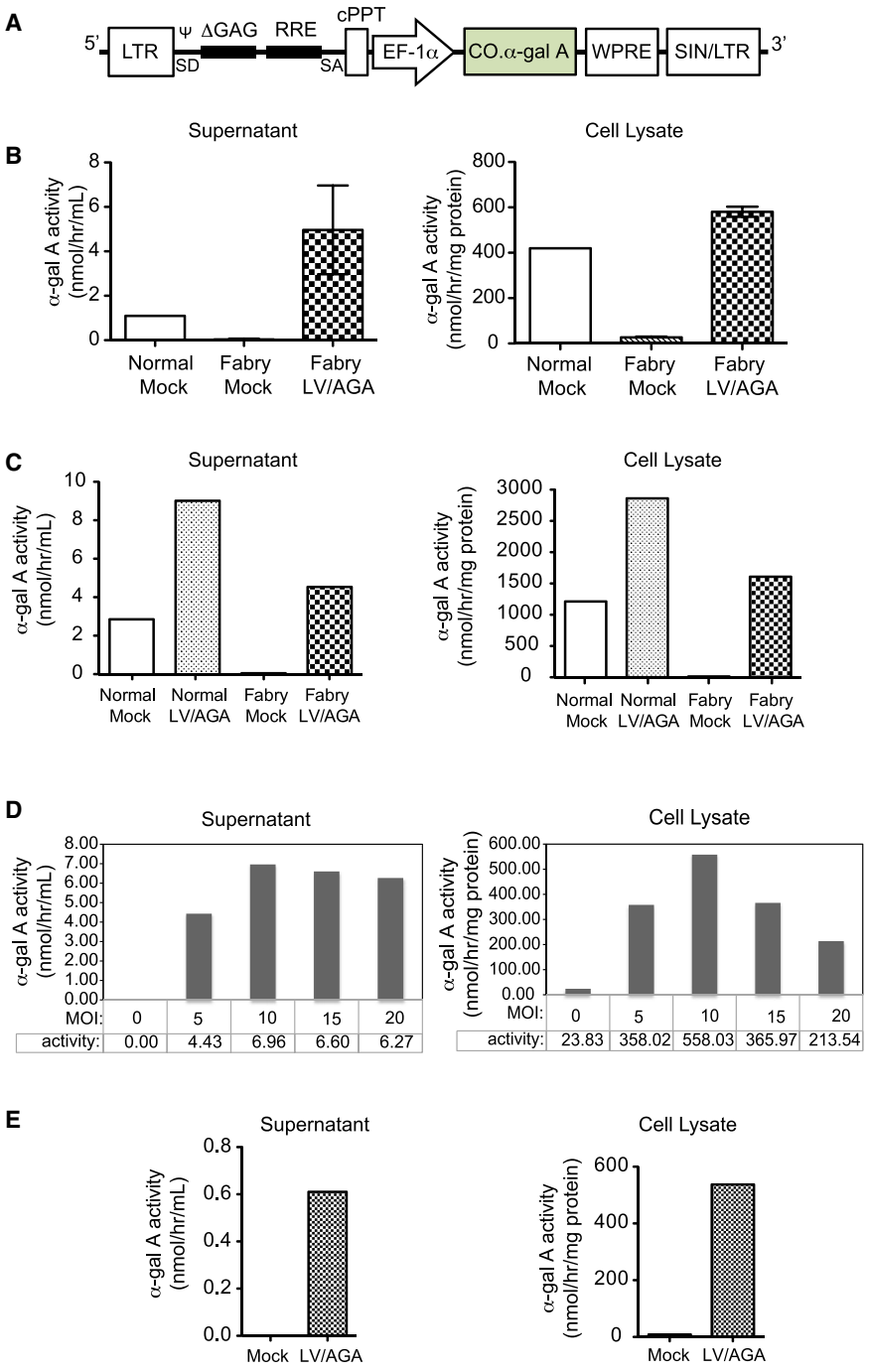

Figure 1. Efficient Transduction of Mobilized Fabry Patient CD34⁺ Hematopoietic Cells with LV/AGA

(A) Schematic of the LV transfer vector, pDY.CO.α-gal A (i.e., LV/AGA), used in this study. LTR, long terminal repeat; Ψ, HIV packaging signal; SD, 5′ splice donor site; ΔGAG, deleted group antigens; RRE, Rev-responsive element; SA, 3′ splice acceptor site; cPPT, central polypurine tract; EF-1α, elongation factor 1 α promoter; CO.α-gal A, codon-optimized cDNA of the human *GLA* gene encoding the wild-type α-gal A enzyme; WPRE, woodchuck hepatitis virus post-transcriptional regulatory element; SIN/LTR, self-inactivating LTR. (B–E) CD34⁺ hematopoietic cells from a healthy donor (normal) or Fabry patient (no. 14-159) were mock-transduced or transduced with research-grade (B) or near-clinical-grade (C) LV/AGA at an MOI of 10. Cell culture supernatants and cell lysates were processed and assayed for α-gal A activity either 2 days (B and D) or 4 days (C and E) post-transduction as described in Materials and Methods. The data presented in (B) are mean ± range from two independent experiments (n = 1 for normal cells and n = 2 for Fabry cells). (D) Fabry patient (no. 14-159)-mobilized CD34⁺ hematopoietic cells were transduced with the research-grade LV/AGA at MOIs of 0, 5, 10, 15, and 20. α-Gal A activity was measured from cell culture supernatants and cell lysates. (E) Mobilized CD34⁺ hematopoietic cells from a Fabry patient (no. 15-220) were mock-transduced or transduced with the near-clinical-grade LV/AGA, and α-gal A activity was measured as in (C).

transplant (BMT) experiments in a previously established Fabry mouse model.[27] We have performed analogous experiments before but with a different Fabry LV construct.[24] Basically, bone marrow (BM) cells from donor Fabry mice were transduced overnight with vehicle (mock) or research-grade LV/AGA at an MOI of 10. Male recipient Fabry mice were lethally irradiated and injected with 1×10^6 transduced cells via their tail veins. Peripheral blood was collected every 4 weeks after BMT. α-Gal A activity was measured in the plasma and in lysates from peripheral blood mononuclear cells (PBMCs) at each collection point. Besides some cases of ulcerative dermatitis, which can happen with lethal irradiation, no untoward effects were observed in recipient animals. Mice infused with LV/AGA-transduced cells (LV/AGA group) had significantly higher α-gal A activity in their plasma throughout 6 months post-BMT compared with mice that received mock-transduced cells (mock group) (Figure 2A). Similarly, α-gal A activity in PBMCs and BM from the mock group was only 3–6 nmol/hr/mg protein but reached 30–35 nmol/hr/mg protein in PBMCs and 120–220 nmol/hr/mg protein in BM of the LV/AGA-treated group (Figure 2B). To ascertain whether organs in transplanted Fabry mice were corrected by transplantation of LV-modified BM cells, we harvested spleens, livers, hearts, and kidneys at 3-month and 6-month endpoints and measured α-gal A activity in tissue lysates. Lysates from the mock group all showed minimal α-gal A activity, whereas spleen, liver, and heart extracts from the LV/AGA group displayed significant elevations in α-gal A activity, ranging from a 10- to 20-fold increase in spleens to a 17- to 47-fold increase in livers and a 10-fold increase in hearts (Figure 2C). In contrast, no α-gal A activity

Table 1. VCN and Transduction Efficiency in Small-Scale LV/AGA-Transduced Cells

	Patient (No. 14-159)				Patient (No. 15-220)	
Samples	Normal Mock	Normal LV/AGA	Fabry Mock	Fabry LV/AGA	Fabry Mock	Fabry LV/AGA
VCN/genome	0	0.25	0	0.43	0	0.33
Percentage of transduced cells by CFC	N/A	N/A	N/A	46	N/A	20

differences were observed in tissue lysates from the kidneys (Figure 2D).

To examine whether transplantation of Fabry mice with LV/AGA-transduced BM cells corrected substrate accumulation, we measured total Gb_3 levels in harvested organs by ultra-performance liquid chromatography tandem MS (UPLC-MS/MS). Representative chromatograms of 22 Gb_3 isoforms analyzed from Fabry mouse spleen tissue are shown in Figure S2. Consistent with elevated α-gal A activity in spleens, livers, and hearts, total Gb_3 levels in these organs were significantly reduced from 1,000–4,000 (area/area internal standard [IS]) in mice from the mock group to ~40–250 (area/area IS) in mice from the LV/AGA-treated group (Figure 2D). Gb_3 levels in kidney extracts from the LV/AGA group also trended toward a decrease compared with the mock group, although the reduction was not statistically significant. These results demonstrated that LV/AGA was safe and engineered expression of functional α-gal A in LV/AGA BMT-treated Fabry mice for up to 6 months (the endpoint of the study); expression of this transgene also efficiently reduced Gb_3 levels in several major organs.

To evaluate the long-term in vivo persistence of LV/AGA integration in transduced cells, we examined average VCN in collected PBMCs, BM, and organs from the Fabry mouse-to-mouse transplant experiments after cells/tissues were lysed and genomic DNA was extracted (Materials and Methods). An average of 0.5–1.5 VCN/genome was detected in PBMCs and BM at each time point up to 6 months post-transplantation (the endpoint of the study). Cells from the spleen had ~0.5 VCN/genome, cells from the liver and heart had 0.1–0.2 VCN/genome, and cells from the kidney had ~0.05 VCN/genome. These results are consistent with the α-gal A activity results: organs with higher VCNs showed higher enzyme activity.

Testing the Safety and Efficacy of LV/AGA-Transduced, Mobilized Fabry Patient CD34⁺ Hematopoietic Cells In Vivo in an NSF Xenograft Model

Our group previously established the NSF mouse model, which is immunodeficient and lacks α-gal A activity.[15] Our previous study demonstrated successful xenotransplantation of normal human $CD34^+$ hematopoietic cells in this mouse model.[15] To examine whether LV/AGA-transduced Fabry patient $CD34^+$ hematopoietic cells could persist and produce functional α-gal A activity in vivo, we carried out xenograft experiments in our NSF mice. Mice were preconditioned by semi-lethal irradiation and injected intraperitoneally with a monoclonal antibody raised against mouse CD122 to deplete natural killer (NK) cells.[15] Then mice were infused with mock or near-clinical-grade LV/AGA-transduced Fabry patient (no. 15-220) $CD34^+$ hematopoietic cells via tail vein injections. Human cell engraftment efficiencies were determined by staining isolated PBMCs or BM from the mice with an antibody against human CD45 (hCD45) followed by flow cytometry analyses. An average of 5%–10% $hCD45^+$ cells were detected in the peripheral blood, and 17%–20% $hCD45^+$ cells were detected in the BM at the study endpoint (Figures 3A and 3B). In addition, around 2% $hCD34^+$ progenitor cells were present in the BM 12 weeks after transplant (Figure 3C). Overall, the human cell engraftment rate was very similar between the animals receiving mock and LV/AGA-transduced Fabry patient cells.

To investigate whether LV/AGA-transduced Fabry patient $CD34^+$ hematopoietic cells produced a functional transgene product in the xenotransplanted NSF mice, we measured α-gal A activity in the plasma, BM, and major organs of recipient animals. The LV/AGA group had significantly higher α-gal A activity in the plasma than the mock group 6 weeks after transplant (Figure 4A). The α-gal A level peaked at 6 weeks and gradually dropped after that (Figure 4A), suggesting rejection of the human cells by these mice because mature NK cells are eventually re-generated. Levels of α-gal A activity in the BM, spleen, and liver from the LV/AGA xenotransplanted group also significantly increased 20-fold, 2.5-fold, and 3.0-fold, respectively, compared with the mock group (Figure 4B). Note that one animal from the mock group was found with a lymphoma at the experimental endpoint. α-Gal A activity in the plasma and in kidney lysates from this animal were abnormally higher than in other mice from the mock group at the study endpoint. The corresponding data points derived from that animal for each tissue are circled in Figures 4A and 4C.

In agreement with the increased α-gal A activity, total Gb_3 levels from the LV/AGA-transplanted group significantly decreased in the spleen and liver compared with the mock group. A trend toward Gb_3 reduction was also found in hearts and kidneys, although these reductions were not statistically significant (Figure 4D). Transduced cells maintaining proviral integration persisted up to 12 weeks post-transplant (i.e., the endpoint of the study); an average of 0.2 VCN/genome was detected in BM cells from the LV/AGA-treated group of mice. Meanwhile, spleen cells showed ~0.02 VCN per genome. Viral copy numbers from livers, hearts, and kidneys were undetectable; i.e., indistinguishable from the mock group (Figure 4E).

These results demonstrated that Fabry patient $CD34^+$ hematopoietic cells transduced with the near-clinical-grade therapeutic LV

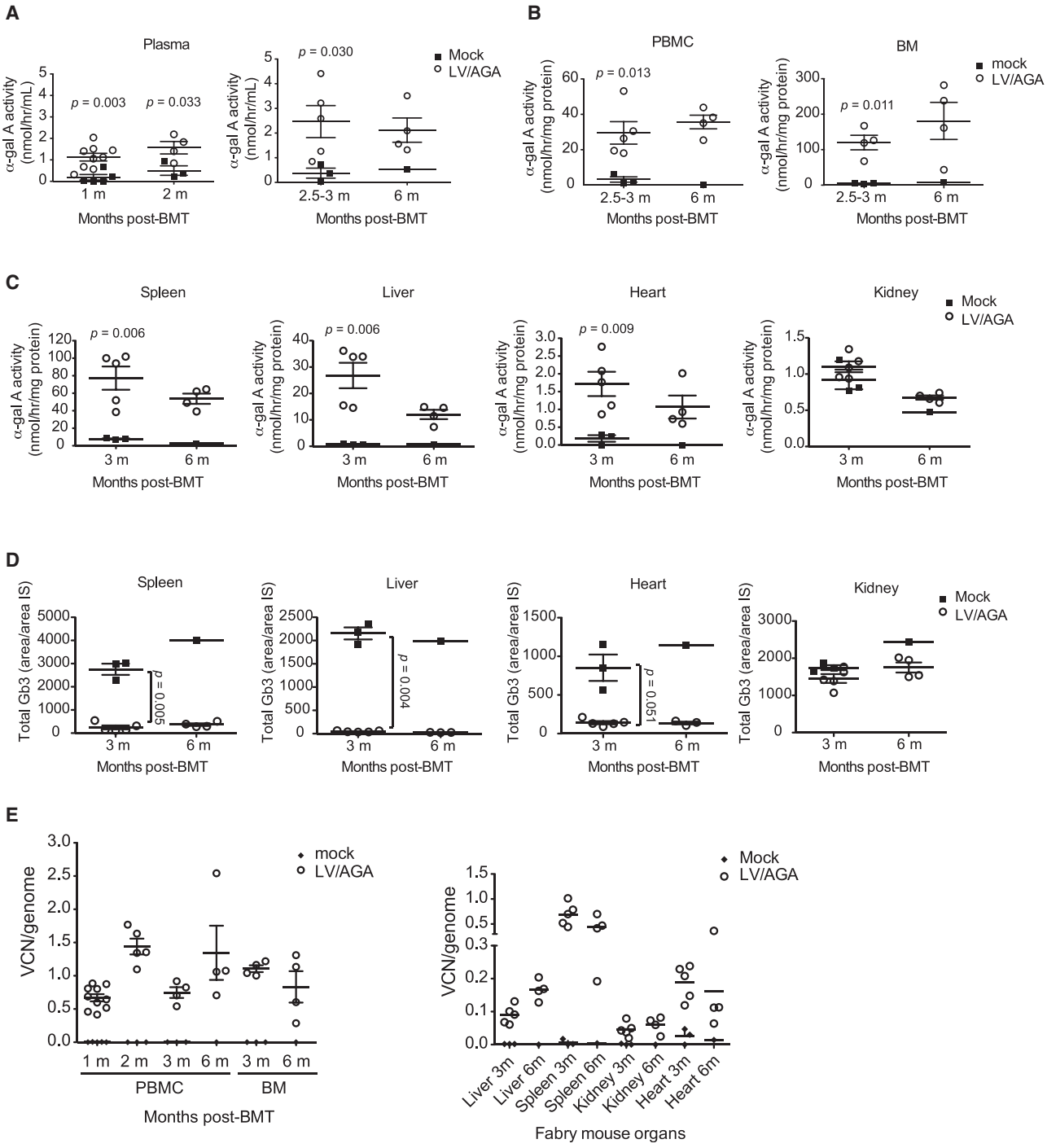

Figure 2. In Vivo Correction of α-Gal A Deficiency by LV/AGA-Engineered Expression of Human α-Gal A in a Fabry Mouse-to-Fabry Mouse BMT Model

BM cells were harvested from donor Fabry mice, and BMMNCs were isolated as described in Materials and Methods. BMMNCs were transduced with vehicle (mock) or LV/AGA and subsequently injected into lethally irradiated recipient Fabry male mice via the tail vein. Peripheral blood was collected every month (m) after transplantation. Half of the mice receiving LV/AGA-transduced cells were killed 3 months post-transplant, and the other half were killed 6 months post-transplant. (A–D) α-Gal A activity from plasma (A), PBMCs and BM (B), and four major organs (C) was determined, and total Gb3 levels in tissues from the organs (D) were measured by mass spectrometry as described in Materials and Methods. Error bars show ± SEM. Data from the mock-transduced group of mice were compared with the LV/AGA-transduced group at each time point, and only p values that were less than 0.05 are shown. (E) Average VCN per genome from PBMCs, BM, and organs of all mice at different collection points was determined by quantitative real-time PCR as described in Materials and Methods.

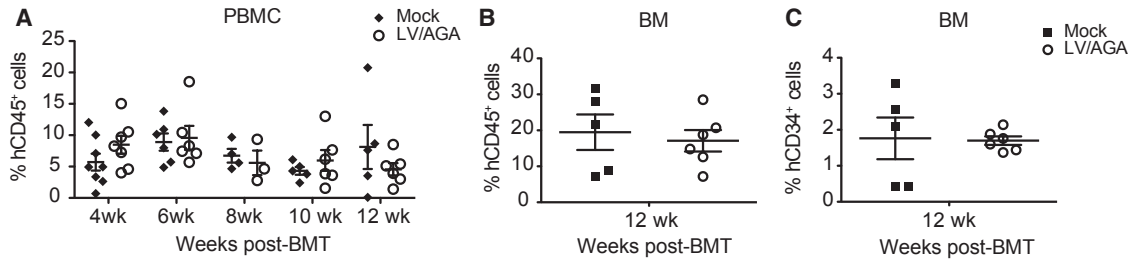

Figure 3. Engraftment of Fabry Patient CD34⁺ Hematopoietic Cells in NSF Mice

(A–C) Mobilized CD34⁺ hematopoietic cells from Fabry patient no. 15-220 were mock-transduced (mock) or transduced with the near-clinical-grade LV/AGA and then injected into conditioned male NSF mice. Peripheral blood was collected 4 weeks (wk) post-transplant and every 2 weeks after that until the mice were terminated 12 weeks after transplant. PBMCs (A) and BM cells (B and C) were stained with PE-conjugated anti-human CD45 antibody or PE-labeled anti-human CD34 antibody, and the percentage of CD45⁺ or CD34⁺ cells was quantified by flow cytometry. Error bar: mean ± SEM.

produced by the IUVPF produced functional α-gal A enzyme in xenotransplanted mice sufficient to correct Gb_3 accumulation in spleens and livers with only an ~20% BM engraftment rate.

LV Integration Profile and Genotoxicity Analysis

An in vitro immortalization (IVIM) assay was performed to test the potential genotoxicity of our therapeutically directed LV vector. This is an insertional mutagenesis assay that evaluates the transformation potential of candidate recombinant lentiviruses. The LV that we tested was LV/FAB, which engineers expression of a cell fate control cassette (ΔLNGFR/TMPK)[16] upstream of the codon-optimized cDNA of the *GLA* gene in a bicistronic format.[16] This vector is an early-version LV designed by our group that has the identical backbone as our current therapeutic version, LV/AGA, plus the IRES element and our patented cell-fate control element.

Two rounds of transduction into primary murine lineage marker-negative (Lin−) BM cells were performed to reach 2–10 VCN/genome. The vectors selected for this assay included LV/FAB, control LV/RRL.PPT.SF.eGFP.pre* (lv-SF), which is a self-inactivating vector expressing EGFP under the control of the strong internal retroviral enhancer/promoter from the spleen focus-forming virus, and a positive control γ-retroviral vector, pRSF91.GFPgPRE (RSF91).[28] After 15 days of culture, transduced cells were diluted and reseeded at low cell density. A 3-(4,5-dimethylthiazol-2-yl)-2,5-diphenyltetrazolium bromide (MTT) assay was performed after 2 additional weeks of clonal expansion as described in Materials and Methods.

Replating frequency (RF) was calculated from the wells demonstrating clonal expansion in each assay (Materials and Methods). No clonal expansion was observed from mock-transduced cells. In contrast, cells transduced with the positive control vectors RSF91 (0.0016 RF/VCN) and lv-SF-(0.000091 RF/VCN) displayed robust transformation.[28] More importantly, cells transduced with LV/FAB only displayed ~0.000036 RF/VCN, 40-fold lower than Lin^- cells transduced with the γ-retroviral vector RSF91 and at the limit of detection of the assay. Furthermore, the incidence of positively scoring assays was significantly lower for LV/FAB compared with control lv-SF.

Genomic DNA was extracted from highly proliferating LV/FAB-transduced cells for linear amplification-mediated PCR (LAM-PCR) analysis as described elsewhere.[28] A non-specific background smear was observed from DNA isolated from mock-transduced cells (Figure 5A). DNA isolated from three of five expanded clones (clones 3, 4, and 5 corresponding to gel lanes 1, 2, and 3, respectively) generated multiple bands on the gel, suggesting random viral integration. Two other clones (clones 6 and 7 corresponding to gel lanes 4 and 5, respectively) did not yield prominent bands. DNA bands from clones 3, 4, and 5 were cut from the gel, purified, and sequenced. As shown in Figure 5A, the DNA bands labeled with red numbers showed low sequencing quality and had no clear match to the murine genome or they matched the vector backbone sequence. Green numbers indicate successful BLAST results for identification of the integration sites. The sequencing results, including Entrez Gene ID, the chromosomal location, raw distance of the insertion site to the next gene, and distance to the transcriptional start site (TSS) of that gene, are listed in Table S1.

Validation of LV Transduction Scale-Up and Cell Production under GMP Conditions

To fulfill the requirements for clinical implementation, we developed an LV/AGA scaled-up transduction protocol under GMP conditions at the UHN Philip S. Orsino Cell Therapy Facility. Fifty million cryopreserved Fabry patient (no. 15-220) $CD34^+$ hematopoietic cells were thawed and cultured in stem cell growth medium (SCGM) supplemented with GMP-grade cytokines in a VueLife cell culture bag at a density of 1×10^6 cells/mL for 24 hr. Then the near-clinical-grade LV/AGA was added to the cell culture to reach an MOI of 10. After overnight transduction, cells were washed twice with Plasma-Lyte A plus 0.5% human serum. Two million cells were split off and placed in complete SCGM (cSCGM) for additional analyses. The remaining cells were pelleted and resuspended in a cryopreservation solution, CryoStor CS10, to maintain a cell density of $2–10 \times 10^6$ cells/mL. The final cell suspension was cryopreserved in an OriGen CryoStore freezing bag and stored in the vapor phase of the liquid nitrogen tank. Quality control (QC) tests were performed on aliquots of the final cell product to ensure that the standards of cell therapy products were met.

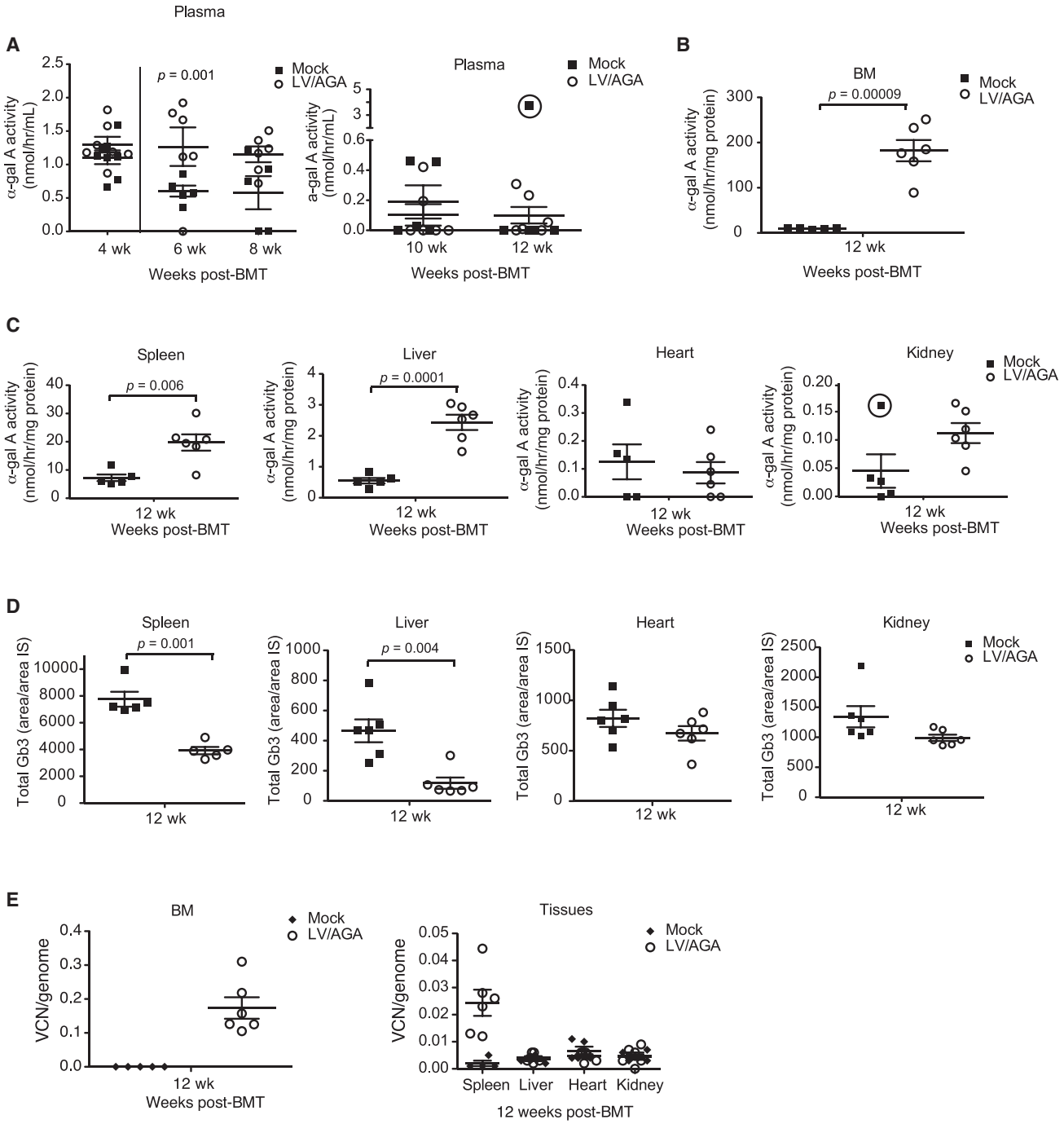

Figure 4. In Vivo Correction of α-Gal A Deficiency by Xenotransplanted LV/AGA-Transduced Fabry Patient CD34⁺ Hematopoietic Cells in NSF Mice

α-Gal A activity in plasma (A), BM (B), and four major organs (C) from NSF mice described in Figure 3 was measured by enzyme assay, and total Gb3 levels in the organs (D) were measured by mass spectrometry as described in Materials and Methods. Bars show ± SEM. The data from the mock group mice were compared with the LV/AGA group at each time point, and only p values that were less than 0.05 are shown. Negative α-gal A activity obtained from several plasma samples is presented as 0 nmol/hr/mL and was not included in the statistical analysis. The total Gb_3 level is the sum of relative abundances of different Gb_3 isoforms, which were expressed as their peak areas divided by the peak area of the internal standard (area/area IS) as described in Materials and Methods. (E) Average VCN per genome from BM and organs of all mice at different collection points was determined by quantitative real-time PCR as described in Materials and Methods.

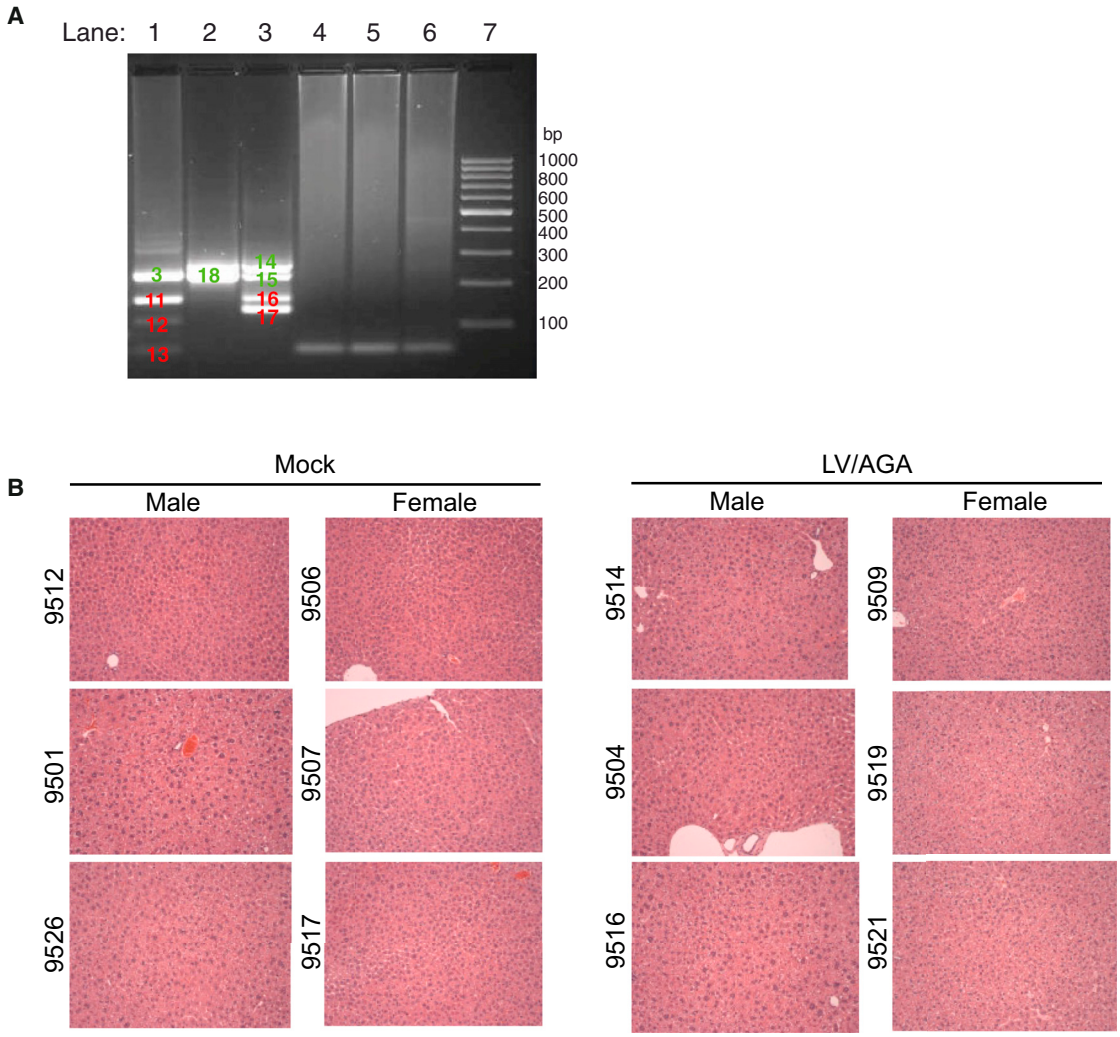

Figure 5. In Vitro Genotoxicity of LV/FAB and In Vivo Toxicity in Livers of NSF Mice Xenotransplanted with LV/AGA-Transduced Mobilized Fabry Patient CD34⁺ Hematopoietic Cells

An IVIM assay was carried out to examine the in vitro genotoxicity of LV/FAB as described in Materials and Methods. (A) The five clones from LV/FAB-transduced mouse BM cells that showed growth were analyzed by LAM-PCR. PCR products were run on a 2% agarose gel (lanes 1–5, clones 3–7; lane 6, mock; lane 7, 1-kb DNA ladder). Prominent DNA bands were cut out and sequenced. Bands with green numbers show that the sequence was identified by BLAST in the mouse genome; bands with red numbers show that the sequence had low quality or no match to the mouse genome. (B) The toxicology study in NSF mice was carried out as described in Materials and Methods. Organs collected on day 7 or day 28 post-transplantation were fixed, sectioned, and stained with H&E for microscopic evaluation. Liver sections from all animals were evaluated for signs of hepatic injury, inflammation, neoplasia and/or degeneration. Representative images of liver sections are shown with each mouse code number next to each image. H&E magnification 100×.

A portion of the 2×10^6 cells harvested post-transduction was subjected to a CFC assay; the remaining cells were kept in culture for 4 more days. Supernatants and a cell pellet were then collected and tested for α-gal A activity as well as for an average VCN per cell. We carried out two independent validation runs (engineering runs) following the above protocol utilizing our approved standard operating procedures (SOPs). The results of the corresponding analyses are listed in Table 2. Total cell viability during the 3-day processes was maintained at 90% and above. The long-term transduction efficiency as evaluated by CFC assay was found to be 67.9% from the first engineering run and 29.8% from the second. A similar viral integration frequency was observed from both runs, an average of 0.59 VCN/genome from the first run and 0.51 VCN/genome from the second. α-Gal A activity levels in both the culture supernatant and lysates were much higher than basal activity levels in non-transduced cells (Table 2; Figure 1D). These results indicated successful scale-up clinical transductions with mobilized Fabry patient CD34⁺ hematopoietic cells.

Finally, to test the stability of the cryopreserved cell product, we thawed the cell product after 1-week storage in vapor phase liquid

Table 2. Analysis of Scale-up Transduction of Fabry Patient CD34⁺ Cells

Analysis	Eng. Run 1	Eng. Run 2
VCN/genome	0.59	0.51
Percentage of transduced cells by CFC	67.9	29.8
α-Gal A activity in supernatant (nmol/hr/mL)	13.15	63.0
α-Gal A activity in cell pellet (nmol/hr/mg protein)	1,888.14	6,517.8
Cell viability during cell processing (%)		
Day 1 (at thaw)	98	96.6
Day 2 (before transduction)	92.5	91.5
Day 3 (before resuspension in freezing medium)	97	89.5

Eng. Run, engineering run.

nitrogen and examined cell viability up to 24 hr post-thawing. The viability of the thawed cells was maintained above 80% up to 6 hr post-thawing but decreased below 80% at 24 hr post-thawing from both engineering runs (Table 3).

In Vivo Toxicology Study of Our Therapeutic Product: LV/AGA-Transduced Fabry Patient CD34⁺ Hematopoietic Cells

To investigate the potential in vivo toxicity of the LV/AGA-transduced Fabry patient CD34⁺ hematopoietic cell product, we used our NSF mouse model for an additional xenograft study. To do this under optimal conditions, the NSF mouse line was re-derived at the Toronto Centre for Phenogenomics (TCP) behind a barrier, and a cohort of 7-week-old mixed-gender mice was selected for these experiments. CD34⁺ hematopoietic cells isolated from a Fabry patient (no. 15-220) were transduced overnight with vehicle (mock) or LV/AGA at an MOI of 10, and 1×10^6 cells were infused into recipient mice 1 day after they were irradiated and treated with antibody against mouse CD122.[15] Half of the mice were killed on day 7, and the remainder were killed on day 28. Mouse weight, body and dermal condition, general appearance, behavior, metabolic parameters, and complete blood counts were assessed.

No overt differences were observed between male and female mice at any of the time points; consequently, the data were pooled from both genders. All mice displayed normal weight gain and dermal condition throughout the course of these analyses. Two LV/AGA group male mice displayed hyperactivity and nervous behavior, whereas all other mice were normal. Four LV/AGA group male mice had ruffled fur, and two LV/AGA group male mice showed ruffled fur as well as a slightly hunched posture. Two LV/AGA group females displayed ruffled fur. One mock group animal had ruffled fur and a slightly hunched posture. Analyses of biochemical parameters revealed that the mice with ruffled fur and a hunched posture had elevated levels of alanine aminotransferase (ALT), aspartate aminotransferase (AST), and total bilirubin, suggesting that mild liver damage occurred in both LV/AGA-treated and mock-treated animals. Analyses of liver histology showed no abnormalities in either group of mice and no obvious difference between groups (Figure 5B), except in liver sections from one animal from the LV/AGA group, where there was a focal area of acute subcapsular hepatic hemorrhage (data not shown). This change was interpreted to be most consistent with terminal handling and unrelated to gene therapy treatment.

Analyses of blood biochemistry parameters revealed no significant differences between mock and LV/AGA mice on either day 7 or day 28 (Table S2). Urinary glucose, urinary nitrite, urinary protein, blood hemoglobin, and urinary leukocytes were examined on days −2, 7, and 28. No overt differences in any of these parameters were observed at any time points in mock or LV/AGA group mice (data not shown).

Both LV/AGA and mock control mice displayed typical radiation-induced cytopenia on day 7 (Table S3). Interestingly, LV/AGA mice had increased platelets compared with mock-transplanted controls on Day 7 (Figure S3A). Whether the radiation-induced nadir was lower or the timeline of platelet recovery was altered is difficult to ascertain with a single time point. Parallel decreases in erythrocytes, lymphocytes, neutrophils, monocytes, basophils, and eosinophils were observed in all animals.

LV/AGA mice displayed slight anemia on day 28. Both LV/AGA and mock mice had elevated red blood cell (RBC) distribution width on day 28. Thrombocytopenia was observed in both groups of mice on day 28. Control mice had lower numbers of lymphocytes, neutrophils, and monocytes on day 28, suggesting that these animals had not recovered as quickly from cytopenia associated with radiation and the subsequent BMT (Table S4; Figure S3B). In sum, no significant toxic effects were observed in NSF mice receiving LV/AGA-transduced Fabry patient CD34⁺ hematopoietic cells.

DISCUSSION

ERT for Fabry disease still has substantial limitations. Intravenous enzyme infusions are required every 2 weeks for life. The procedure time and travel to an infusion center or hospital along with chronic intravenous access issues (in some patients a permanent in-dwelling catheter is surgically inserted) are problematic. In Canada, the costs of ERT alone can exceed $300,000/patient/year. Inactivating antibodies can also develop against the infused product that could theoretically limit drug action. To date, five randomized, placebo-controlled ERT trials in a total of 239 patients, with extension trials and data from multi-national registries of Fabry patients, have shown only modest improvements in left ventricular mass, stabilization of renal function, quality of life, lessening of neuropathic pain, and reduction of Gb_3 in tissues, plasma, and urine.[29–37]

Gene therapy has the potential to offer a sustained therapeutic response in Fabry disease with a minimal number of treatments and lower costs. Trials have been undertaken in children in Milan for two other lysosomal storage disorders (LSDs) to examine feasibility/safety; patients have been treated by LV-mediated gene transfer targeting primitive hematopoietic cells for metachromatic leukodystrophy (MLD)[38] and globoid cell leukodystrophy (GLD).[39] The results from the MLD trial have demonstrated short-term safety and

Table 3. Stability of the Cryopreserved Cell Product

	At Thaw	Time after Thaw (hr)						
Time of Cell Counting		1	2	3	4	5	6	24
Eng. run 1 cell viability (%)	98.6	97.8	97.2	94.9	89.1	94.5	96.1	58.1
Eng. run 2 cell viability (%)	83	90.7	90.9	88.2	89.2	82.2	86.9	78.2

a high sustained level of gene marking and associated enzyme activity.[38]

Previous studies from our group demonstrated long-term enzyme correction and lipid reductions in Fabry mice treated with direct injections of a recombinant LV engineering expression of α-gal A[26] or with LV-transduced murine HSCs.[24] In the latter study, even low MOIs led to high levels of intracellular and secreted α-gal A activity. Organ enzyme activity was high 24 weeks after transplant of LV-transduced mouse BM cells, and secondary transplants led to increased α-gal A activity a full 20 weeks after infusion of cells from donor animals.[24] We have also shown successful engraftment of LV-transduced human normal $CD34^+$ hematopoietic cells in NSF mice and α-gal A correction in several major organs.[15] To evaluate gene therapy for treating Fabry patients, we are initiating a first-in-the-world pilot gene therapy trial for Fabry disease.

Because the primary endpoint of our clinical study is the evaluation of the safety of this approach, we originally designed a bicistronic vector, LV/FAB (and LV/FAB-2), containing a cell-fate control element that can selectively eliminate transduced cells if they become oncogenic in vivo.[16] Meanwhile, we examined the viral integration profile in genomes of transduced mouse BM progenitor cells, and LV/FAB showed a significantly lower risk of inducing clonal outgrowth than a control γ-retroviral vector or another lentivector (lv-SF) that uses the strong internal retroviral enhancer/promoter from the spleen focus-forming virus.

The functionality of our clinically directed LV is another important factor for our proposed trial because the systemic therapeutic effect depends on the level of α-gal A expression from the transduced patient $CD34^+$ hematopoietic cells. Fabry patient $CD34^+$ hematopoietic cells transduced with LV/FAB only produced a 10%–20% α-gal A activity level of that from normal $CD34^+$ cells, however. To improve the vector efficacy, we optimized the consensus Kozak sequence in the transfer vector for LV/FAB and made another LV/α-gal, A.IRES.hCD25, in which the cDNA encoding α-gal A is directly under the control of the EF-1α promoter. It turned out that Fabry patient $CD34^+$ hematopoietic cells transduced with these vectors still did not express a level of active α-gal A activity comparable with normal cells. We speculated that the IRES-mediated bicistronic system might negatively affect the expression of α-gal A. Therefore, finally, we constructed a simple transfer vector with only a codon-optimized human cDNA encoding α-gal A as the transgene. The resulting LV/AGA showed much better efficacy because LV-transduced Fabry patient $CD34^+$ cells produced higher-than-normal cell levels of α-gal A activity. We further investigated the efficacy of LV/AGA in Fabry patient $CD34^+$ hematopoietic cells both ex vivo and in a xenotransplant mouse model. This shows, for the first time, that the therapeutic product, LV/AGA-transduced Fabry patient $CD34^+$ hematopoietic cells, produced functional α-gal A activity in an animal model and achieved enzyme correction and lipid reduction in tissues. The development of the safe and efficient clinically directed LV/AGA and pre-clinical results from it were critical for approval of our pilot gene therapy trial for the treatment of Fabry patients.

There was no overt LV/AGA-related toxicity observed in any murine experiments except possible immunogenicity-related reactions against the human protein. In the Fabry mouse-to mouse transplant experiment, we observed that one mouse from the LV/AGA group spontaneously died 9 weeks after transplant. This mouse developed ulcerative skin dermatitis on the neck and top back. We also observed various degrees of ulcerative dermatitis and ulcerative cornea in four of five mice from the mock group and six of ten mice from the LV/AGA group. Two mice from the LV/AGA group showed more severe ulcers and had to be euthanized around 10 weeks after transplant according to our UHN animal use protocol. These symptoms were also observed in mice from the mock group that received donor cells without LV transduction. Therefore, the ulcerative phenomenon is likely caused by irradiation or our transplantation protocol itself. The relatively more severe ulcerative pathology in the LV/AGA group mice may be due to manifestations of graft-versus-host disease because these mice received cells that express human α-gal A, and the research-grade LV prep we used for this study may also contain residual host cell (HEK293T) protein and DNA that is immunogenic to mice. The ulcerative dermatitis symptom was not observed in the NSF mice xenotransplant experiment, in which the mice are immunodeficient and transplanted cells were transduced with the near-clinical grade LV that has minimal host cell contaminants, as analyzed/approved by QC tests. In these NSF mice, we observed that two mice from the mock group and two mice from the LV/AGA group spontaneously died within 1 month after transplant, possibly because of inefficient engraftment or accidental infections in these mice. One mouse from the mock group was very sick ~6 weeks post-transplant and was euthanized prematurely according to the UHN animal use protocol. All other mice remained healthy until the endpoint, when they were terminated for tissue collection.

We also performed IVIM experiments to investigate possible genotoxicity caused by LV integration. A caveat of this approach is that higher MOIs than we are planning for the actual clinical trial are necessary to perform an exhaustive insertion site analysis in concert

with high-throughput sequencing. Four clones were successfully sequenced from LV/FAB-transduced murine cells and showed clear identity in the mouse genome. Two intronic inserts were observed in mouse chromosome 10 for LV/FAB-transduced samples. Insertion in *PDE7B* (phosphodiesterase 7B; sequence 3, lane 1) is closest to *AHI1* (Abelson helper integration site-1) for which we observed an intronic hit in sequence 18 (lane 2). The *AHI1* gene belongs to a family of modular proteins containing one SH3 motif and seven WD40 repeats. *AHI1* was originally identified as a target of proviral integration in murine leukemia[40] and is a target of retroviral mutagenesis.[41] Jiang et al.[41] have shown that *AHI1* collaborates with BCR-ABL in a mouse model of leukemogenesis. Although *Ahi1* has been shown to play a role in mouse leukemogenesis, there is limited evidence that mutation of *AHI1* is relevant in human cancer. Only one mutation, T1034A, has been documented in two patients in 2,139 sequencing studies reported in hematopoietic and lymphoid malignancies deposited in the online database Catalogue of Somatic Mutations in Cancer (COSMIC). Biallelic mutation of *AHI1* has been documented in consanguineous families, leading to Joubert syndrome (JBTS3), marked by hypotonia and developmental delay, among other symptoms.[42,43]

Two fragments of the same insertion site were identified upstream of *HEY1* (lane 3, sequences 14 and 17). *HEY1* (hairy/enhancer-of-split related with YRPW motif 1) is a downstream target of Notch signaling.[44] The related family member, *HEY2*, maps adjacent to *HEY1* on mouse chromosome 3. The two *Hey* genes play a redundant role in facilitating Notch-dependent signals.[44] *HEY1-NCOA2* chromosomal translocations are observed in human mesenchymal chondrosarcomas.[45] *HEY1* provides a helix-loop-helix oligomerization interface and is not transcriptionally active in this setting. There is no evidence for mutation of *HEY1* in hematopoietic or lymphoid neoplasms in the 2,139 studies deposited in COSMIC. Although the NOTCH pathway plays a role in T cell-mediated acute lymphoid leukemia, it is unclear what the function of a low-frequency integration into the *HEY1* locus would be. Although integration into loci with a documented role in oncology was observed in the IVIM assay, it is important to note that the events occurred in intragenic or intronic regions, in keeping with published studies indicating that LVs do not preferentially integrate into promoter regions,[38,46,47] a clear improvement over previous oncoretroviral strategies.

LV-mediated gene delivery has several advantages over previous delivery platforms. Most notably, LVs have been demonstrated to be safe in the clinic to date. We have selected Fabry disease for an initial clinical study because we believe that wide ranges of α-gal A expression are very well tolerated and that patients with Fabry disease mainly lack primary CNS symptoms. In this study, we showed that therapeutic LV/AGA-transduced patient $CD34^+$ hematopoietic cells produce efficient functional α-gal A activity and displayed minimal toxicity in two different mouse models. We successfully developed a large-scale ex vivo culture and LV transduction process on Fabry patient $CD34^+$ hematopoietic cells to fulfill pre-clinical requirements. We are confident from these preclinical data that gene therapy holds promise for treatment of this disorder.

MATERIALS AND METHODS

Reagents

Phycoerythrin (PE)-labeled mouse anti-human CD45 and CD34 antibodies along with mouse immunoglobulin 1 (IgG1) κ isotype (all from BD Biosciences) were used for flow cytometry. Anti-mouse CD122 antibody (clone TM-β1) for in vivo depletion of NK cells was purchased from BioLegend. Research-grade human stem cell factor (SCF), FLT3L, thrombopoietin (TPO), interleukin-3 (IL-3), and GMP-grade SCF and IL-3 were from R&D Systems. GMP-grade human FLT3L and TPO were from CellGenix. Recombinant mouse cytokines, SCF, FLT3L, TPO, and IL-6 were from R&D Systems. Human Serum Plus was from GEMINI Bio Products. Trypan blue stain (0.4%), fetal bovine serum, and goat serum were from Life Technologies. The chemicals used in this study included 5-FU (Sigma-Aldrich), protamine sulfate (Sigma-Aldrich and Fresenius Kabi Canada), NycoPrep 1.077A (AXIS-SHIELD), 4-methylumbelliferyl-α-D-galactopyranoside (Research Products International), N-acetyl-D-galactosamine (Sigma-Aldrich), BSA (BioShop), and Proteinase K (Invitrogen).

N-Octadecanoyl-D3-ceramide trihexoside (Gb3[(d18:1)(C18:0)D3], 98+%), heptadecanoyl-ceramide trihexoside (Gb_3(d18:1)(C17:0), 98+%), and ceramide trihexoside (Gb_3 isoform/analog mixture) were purchased from Matreya. High-performance liquid chromatography (HPLC)-grade tert-butyl methyl ether (MTBE) was from Sigma-Aldrich. HPLC-grade methanol (MeOH) was from EMD Chemicals. Optima liquid chromatography-MS (LC-MS)-grade water, ammonium formate (Amm. Form., 99%), and American Chemical Society (ACS) reagent grades for both glacial acetic acid and potassium hydroxide (KOH) pellets were from Fisher Scientific. Formic acid (FA) (+99%) was from Acros Organics.

Stem Cell Mobilization and Leukapheresis

All studies involving patient samples were approved by the research ethics boards of UHN, Alberta Children's Hospital, and McMaster University. Fabry patients were guided through the informed consent process for this study by qualified personnel at the Alberta Children's Hospital. To collect mobilized peripheral blood $CD34^+$ cells, Fabry patients underwent stem cell mobilization via treatment with Granulocyte Colony Stimulating Factor (G-CSF, aka Neupogen, AMGEN) using standard of care procedures offered at the Foothills Medical Center. A dosage of 16 μg/kg G-CSF was administered intravenously daily for 4 days prior to collection and on each day of collection for a maximum of 3 days.

Leukapheresis was carried out through patient central or peripheral venous access using a Spectra Optia system (Terumo BCT) according to the SOP for collection of stem cell products at the Foothills Medical Center. Mononuclear cells were collected into sterile leukapheresis bags. At the end of each collection day, harvested cells were stored in a temperature-controlled cooler and transported on the same

day to the Juravinski Cancer Centre. A total of 3 continuous days of collection was performed for each patient; day 1 and day 2 collections were transported to the Juravinski Cancer Centre for $CD34^+$ stem/progenitor cell isolation.

Isolation of $CD34^+$ Cells from the Leukapheresis Product

A CliniMACS $CD34^+$ reagent system (Miltenyi Biotec) was used to isolate $CD34^+$ hematopoietic stem/progenitor cells at the Juravinski Cancer Centre (using established SOPs) from the leukapheresis product harvested on the previous day. After magnetic labeling with an anti-human CD34 antibody, the $CD34^+$ hematopoietic cells were enriched using a high-gradient magnetic separation column connected to a closed disposable tubing set. After washing steps, the retained $CD34^+$ hematopoietic cells were eluted by removal of the magnetic field. The degree of purification was monitored by flow cytometry analysis after staining an aliquot of purified product with a two-color fluorescein isothiocyanate (FITC)-CD45/PE-CD34 reagent from the Stem-Kit (Beckman Coulter).

Isolated $CD34^+$ cells were immediately resuspended in 10% Cryoserv DMSO (Bioniche PHARMA) plus 10% autologous plasma and 80% Plasma-Lyte A (Baxter) in CryoStore freezing bags (OriGen Biomedical) and cryopreserved using a controlled-rate freezer (Planer). Following this, the cells were stored in the vapor phase of a liquid nitrogen tank. The cryopreserved $CD34^+$ cells were later transported to our laboratory at UHN or directly to the Philip S. Orsino Cell Processing Facility at Princess Margaret Hospital for LV transduction.

Cell Culture

HEK293T cells were cultured in DMEM (Gibco by Life Technologies) supplemented with 10% fetal bovine serum and 1× penicillin-streptomycin-glutamine (PSQ) (2 mM glutamine, 100 U/mL penicillin, and 100 mg/mL streptomycin; Gibco by Life Technologies).

Mobilized peripheral blood normal $CD34^+$ cells from healthy donors were purchased from AllCells. Human primary $CD34^+$ cells were cultured in CellGro stem cell growth medium supplemented with 300 ng/mL recombinant human SCF, 300 ng/mL recombinant human FLT3L, 100 ng/mL human TPO, and 60 ng/mL recombinant human IL-3.

Mouse primary bone marrow PBMCs were cultured in CellGro stem cell growth medium supplemented with 100 ng/mL recombinant mouse SCF, 100 ng/mL recombinant mouse FLT3L, 100 ng/mL mouse TPO, and 10 ng/mL mouse IL-6.

All cells were maintained in a humidified incubator at 37°C with 5% CO_2.

LV Construction

A DNA fragment comprising the Kozak sequence and the cDNA of the human *GLA* gene encoding α-gal A was synthesized by GenScript. The cDNA of the *GLA* gene was codon-optimized for enhanced expression in human cells. The synthesized DNA fragment was subcloned into the 3′ self-inactivating (3′SIN), HIV-1-based, lentiviral backbone pDY.cPPT-EF1α.WPRE previously generated in our laboratory[16] between the EcoRI and XmaI restriction sites to generate the plasmid pDY.CO.α-gal A. We later observed that the Kozak sequence in this construct was not optimal because of a missing guanine nucleotide at the −6 bp position before the start codon. To avoid a potential reduction in gene expression, an optimal Kozak sequence was engineered in the plasmid by site-directed mutagenesis using the Q5 site-directed mutagenesis kit (New England Biolabs). The fixed pDY.CO.α-gal A plasmid was used for all LV preparations in this study. The plasmid sequence covering the proviral region was verified by DNA sequencing.

Purification of Research-Grade and Near-Clinical-Grade LV along with Functional Titer Analyses

Research-grade LV/AGA was prepared in our laboratory at UHN as described previously.[48] Near-clinical-grade LV/AGA was produced at the IUVPF, which meets current GMP requirements for potential human clinical trial use under an investigational new drug (IND) submission. The LV particles were produced using HEK293T packaging cells from a certified master working cell bank maintained by the IUVPF. The packaging cells were expanded to a 4-L culture volume and transiently co-transfected with the LV packaging plasmids (pCMVΔR8.91 and pMDG) and transfer plasmid (pDY.CO.α-gal A) provided by our laboratory. The sequences of those plasmids that were expanded at IUVPF were verified by DNA sequencing at ACGT. Culture supernatant was harvested twice, yielding a total of 8 L of unconcentrated LV-containing supernatant. The LV-containing supernatant was further purified by Mustang Q ion exchange chromatography, concentrated by tangential flow filtration, and buffer-exchanged into ∼100 mL GMP-grade CellGrow stem cell growth medium.

Sample vials of the final concentrated vector product were retained by the IUVPF for QC analyses, including vector identity confirmation by Southern blot analysis and titer by p24 ELISA, along with testing for aerobic and anaerobic sterility, mycoplasma levels, endotoxin levels, and residual DNA benzonase levels.

We performed infectious titer testing at our UHN laboratory on all LV preparations by transduction of HEK293T cells using serial dilutions of the vector followed by measurement of average proviral copy number per cell using quantitative real-time PCR analysis (see below).

LV Transduction

Frozen $CD34^+$ hematopoietic cells from Fabry patients enrolled for this study as well as from healthy donors purchased from AllCell Technologies were quickly thawed at 37°C, washed with SCGM, and cultured in complete SCGM for 24 hr at a density of 1×10^6 cells/mL. For small-scale transductions, cells were pelleted by centrifugation at 300 × *g* for 10 min at room temperature. The cell pellet was then resuspended in complete SCGM containing the LV/AGA preparation and protamine sulfate (final concentration at 8 μg/mL) to reach an MOI of 10 and to maintain a final cell density

of 1×10^6 cells/mL. Cells were put in appropriate sterile culture vessels to keep a (culture volume)/(vessel surface area) ratio of 9.62 cm^2/mL ± 10% to allow consistent contact between LV particles and cells. Cells were incubated in a humidified 37°C and 5% CO_2 incubator overnight, washed, and resuspended in fresh complete growth medium for 2 or 4 more days.

For large-scale transduction experiments carried out in the Philip S. Orsino GMP-compliant facility in Princess Margaret Hospital, 50–80×10^6 cells were thawed and cultured for 24 hr in complete growth medium in VueLife cell culture bags (Saint-Goubain) to maintain the depth of cell suspension between 0.3 and 0.5 cm. Protamine sulfate was added to the cell suspension, mixed, and followed by addition of the near-clinical-grade LV/AGA viral preparation to reach an MOI of 10. After a 16- to 18-hr overnight transduction, cells were transferred into 500-mL conical tubes and centrifuged at $300 \times g$ for 10 min. The cell pellet was resuspended in wash buffer (Plasma-Lyte A containing 0.5% Human Serum Plus) and washed twice to remove residual LV particles. An aliquot of cell suspension was grown for an additional 4 days at our UHN laboratory; culture supernatants and cell pellets were collected at the end of the growth period for α-gal A enzyme assays and qPCR analyses. The remaining post-transduction cells were resuspended in CryoStor CS10 (BioLife Solutions) freezing medium and transferred into CryoStore freezing bags (OriGen Biomedical). Aliquots of the cell product were sampled for QC testing for microbiology (Department of Microbiology, Mount Sinai Hospital) and mycoplasma (WuXi AppTec) sterility, endotoxin level (Endosafe-PTS system, Charles River Laboratories; performed by Translational Immunotherapy Laboratory, Immune Therapy Program, Princess Margaret Hospital) and cell viability (in our laboratory at UHN).

Measurement of α-gal A Activity

The assay used to measure α-gal A activity was described previously.[26] Basically, cells or tissues were lysed by freezing/thawing or by Dounce homogenization in cell homogenization buffer (CHB; 28 mmol/L citric acid, 44 mmol/L disodium phosphate, and 5 mg/mL sodium taurocholate). After centrifugation, clear lysates were incubated with α-gal A substrate solution (5 mmol/L 4-methylumbelliferyl-α-D-galactopyranoside, 100 mmol/L N-acetyl-D-galactosamine, and 4 mg/mL BSA) at 37°C for 1–4 hr. Stop solution (1.1 mol/L glycine and 0.1 mol/L NaOH) was then added to the reaction. The fluorescence from each reaction in a plate was measured on a microtiter plate fluorometer (DYNEX Technologies) with excitation at 350 nm and emission at 460 nm. Serially diluted 4-methylumbelliferone (Sigma-Aldrich) solutions were used as standards. CHB buffer was used as a blank for cell lysates, and heat-inactivated pooled Fabry mouse plasma was used as a blank for plasma samples.

Quantitative Real-Time PCR

Four days after transduction, cells were collected and washed once in PBS. 1×10^6 cells were processed for genomic DNA extraction using the Gentra Puregene cell kit (QIAGEN) according to the manufacturer's instructions. A set of primers (WPRE-RT-F, 5′ TCCTGG TTGCTGTCTCTTTATG 3′; WPRE-RT-R, 5′ TGACAGGTGGTG GCAATG 3′) and a TaqMan probe (5′ FAM-TGCTGACGCA ACCCCCACTGGT-TAMRA 3′, synthesized by Life Technologies) that target a LV-specific region (i.e., the WPRE) were used for the real-time PCR reaction.

Fifty nanograms of genomic DNA prepared from a myeloid cell clone containing one-copy LV integration (established in our laboratory and verified by Southern blot; data not shown) were serially diluted with genomic DNA from a non-transduced clone to generate DNA standards. Real-time PCR was performed on these DNA dilutions to generate a standard curve of cycle threshold (Ct) value versus VCN for quantification of test samples in parallel. The vector copy number in transduced cells (copy number per genome) was determined by plotting the Ct value from transduced cells against the standard curve.

Human β-actin levels were detected with a TaqMan gene expression assay kit (Life Technologies, 4331182, gene ID Hs03023880_g1) and were used to normalize genomic DNA levels between test samples and the standards.

Colony-Forming Cell Assay

After an overnight transduction, $CD34^+$ hematopoietic cells were washed once with SCGM and resuspended in complete SCGM to a density of 1×10^6 cells/mL. 3×10^4 cells were transferred into a 1.5-mL microcentrifuge tube and mixed with 0.3 mL SCGM. The cell suspension was added to a 3-mL MethoCult (STEMCELL Technologies, H4434)-containing sterile tube and mixed thoroughly by vortexing. The mixture was dispensed into two 35-mm sterile culture dishes at 1.1 mL/dish. The dishes were incubated in a humidified 37°C, 5% CO_2 incubator for 2 weeks. Single cell-derived colonies were manually picked under a phase contrast light microscope and lysed in colony lysis buffer (100 mM Tris-HCl [pH 8.5], 5 mM EDTA, 0.2% SDS, 200 mM NaCl, and 0.41 mg/mL Proteinase K). Colony lysates were subjected to endpoint PCR to detect the presence of the LV-specific element, WPRE, with primer sets (WPRE-RT-F2: 5′-TCCTGGTTGCTGTCTCTTTATG-3′ and WPRE-RT-R2: 5′-TG ACAGGTGGTGGCAATG-3′ or WPRE2 FW: 5′CGCTGCTTT AATGCCTTTG 3′and WPRE2 REV: 5′ AAGGGAGATCCGACTCG TCT 3′).

Ultra-Performance Liquid Chromatography/Tandem MS Analysis of Gb_3 Isoforms in Mouse Tissue Samples

A previously validated and published procedure[49] was used for the homogenization, extraction, and MS analysis of Gb_3 isoforms in kidney, liver, spleen, and heart tissue samples from NSF mice. Briefly, tissue samples were homogenized in 400 μL of methanol at high speed (5 m/s) with five zirconium oxide beads (1.4-mm diameter, Omni International) for 45 s using a Bead Ruptor 12 homogenizer (Omni International). Samples were diluted with methanol to reach a concentration of 2.5 mg/mL. Diluted homogenates (1 mL) were spiked with 100 μL of Gb_3[(d18:1)(C18:0)D3] (Matreya, 1 μg/100 μL) internal standard, saponified with KOH (1 M in methanol), and extracted

with MTBE. The organic layers were evaporated to dryness and resuspended in 500 μL of methanol, 5 mM ammonium formate, and 0.1% formic acid. Separation of the Gb_3 isoforms was performed by ultra-performance liquid chromatography (UPLC) (Acquity I-class, Waters) using a hollow structure section (HSS) T3 C18 column (Waters) and analyzed by tandem MS (Xevo TQ-S, Waters) in multiple reaction monitoring (MRM) mode with positive electrospray ionization. Peak areas were measured using QuanLynx V4.1 software (Waters), and relative abundances of different Gb_3 isoforms were expressed as their peak areas divided by the peak area of the internal standard.

Animals

Fabry hemizygous male and Fabry homozygous female mice that are deficient in α-gal A activity were generated previously.[27] NOD/SCID/Fabry (NSF) mice were generated previously by our group.[15] All mice were housed at the Animal Resource Centre at UHN or at the TCP under specific pathogen-free conditions. All animal studies were approved by the UHN and TCP Animal Care Committees.

Isolation of Mouse BMMNCs, LV Transduction, and BMT

BM cells were harvested from mixed-gender donor Fabry mice (8–26 weeks old), and BM mononuclear cells (BMMNCs) were isolated over a Nycoprep 1.077 density gradient as described previously.[24] BMMNCs were washed with RPMI (Sigma-Aldrich) and resuspended in complete RPMI (10% fetal bovine serum [FBS] plus 1× PSQ), and live cells were quantified by trypan blue exclusion. Cells were split into two tubes and centrifuged at 400 × *g* for 10 min. The cell pellet in the first tube was resuspended in complete SCGM (SCGM supplemented with mouse cytokines: 10 ng/mL recombinant mouse (rm)IL-6, 100 ng/mL rmFLT3L, 100 ng/mL rmTPO, and 100 ng/mL rmSCF) and protamine sulfate (8 μg/mL) to reach a cell density of 1×10^6 cells/mL (mock transduction). The cell pellet in the second tube was resuspended in research-grade LV/AGA supplemented with complete SCGM and protamine sulfate to reach a cell density of 1×10^6 cells/mL and MOI of 10 (LV/AGA transduction). Cells were incubated overnight in a humidified incubator at 37°C with 5% CO_2 for the transduction. The next morning, cells were washed, counted, and resuspended in 1× PBS.

One million mock- or LV/AGA-transduced cells were injected via the tail vein into lethally irradiated (11 Gy) recipient Fabry male mice (8–15 weeks old). Recipient Fabry mice were randomized and divided into three groups with 5 mice/group: mock group, mice receiving mock-transduced donor cells; LV/AGA group (short-term), mice receiving LV/AGA-transduced donor cells and sacrificed 12 weeks after transplantation; and LV/AGA group (long-term), mice receiving LV/AGA-transduced donor cells and sacrificed 24 weeks after transplantation.

Peripheral blood was collected from recipient mice by saphenous vein blood draw every 4 weeks after transplant or by cardiac puncture at termination. Plasma and cells were separated by centrifugation at room temperature, and RBCs were lysed with RBC lysis buffer (Sigma-Aldrich) to yield PBMCs.

NSF Mouse Xenotransplantation

NSF male mice (7–10 week old) received less-than-lethal irradiation (3 Gy) and were injected intraperitoneally with a monoclonal antibody against mouse CD122 (200 μg/mouse) to deplete NK cells as described previously.[15] One day later, mice were injected via the tail vein with mock or near clinical-grade LV/AGA-transduced Fabry patient (no. 15-220) $CD34^+$ hematopoietic cells (described in LV Transduction). Mice were randomized and divided into two groups with 8 mice/group: mock group, mice receiving mock-transduced Fabry $CD34^+$ cells; LV/AGA group, mice receiving LV/AGA-transduced Fabry $CD34^+$ cells. Mice were killed 12 weeks after transplant.

For the toxicology study, NSF mice were housed at TCP, and a cohort of 7- to 8-week-old NSF male and female mice was acclimatized for 6 days and subsequently xenotransplanted with Fabry $CD34^+$ hematopoietic cells. Fabry patient (no. 15-220) $CD34^+$ hematopoietic cells were either mock-transduced or transduced with the near-clinical-grade LV/AGA at an MOI of 10 in our laboratory and delivered to TCP on the day of injection. One million cells were injected into each mouse, and we formed two treatment groups: mock group, mice receiving mock-transduced cells; LV/AGA group, mice receiving LV/AGA-transduced cells. All mice were monitored daily, and body weight was measured daily for the first week and once per week thereafter. A clinical assessment was performed weekly and on the day of study termination. Half of the mice in each group were killed on day 7 and the remainder on day 28. On the day of study termination, urine and whole blood were collected for urinalysis, hematology, and plasma chemistry analysis. A target organ panel (brain, heart, lung, liver, spleen, kidney, testes or ovaries, and bone marrow) was collected for snap-freezing in LN_2, followed by complete necropsy with tissue collection for immersion fixation in 10% neutral buffered formalin. Fixed samples were trimmed, embedded in paraffin wax, sectioned, and stained with H&E for microscopic evaluation. The histopathology analyses of each tissue were reviewed by an American Board of Toxicology-certified animal pathologist.

IVIM Assays

IVIM assays were carried out as described previously.[28]

Viral Transduction and Clonal Expansion of Murine BM Cells

Mouse Lin^- BM cells were isolated and kept at −80°C overnight. Cells were thawed the following day and seeded in a 24-well plate at 1×10^5 cells/well in StemSpan medium supplemented with complete growth medium supplement (CGMS; 1% penicillin/streptomycin, 50 ng/mL mouse SCF, 100 ng/mL FLT-3L, 100 ng/mL IL-11, and 20 ng/mL mouse IL-3; all from PeproTech) and incubated for 2 days. Plates coated with Retronectin (Takara Bio) were used to preload viral constructs, and the first round of transduction was completed with prestimulated Lin^- cells. A new Retronectin-coated plate was used for preloading viral vectors on the following day (day 0), and a second round of transduction was conducted by transferring transduced cells to the new plate. After overnight incubation, cells were transferred to 12-well plates and cultured in Iscove's modified Dulbecco's medium (IMDM; Biochrom) supplemented with CGMS. After day 15, cells were seeded at 100 cells/well in 96-well

plates and cultured for an additional 2 weeks. Trypan blue exclusion counting was performed on days 1, 4, 6, 8, 11, and 15.

Measurement of VCN by Quantitative Real-Time PCR

Quantitative real-time PCR analysis was performed using genomic DNA (100 ng) as a template to determine VCN per cell. Samples were analyzed in triplicate. Proviral content was determined from WPRE sequences, and the Ptbp2 gene (genomic reference sequence) was used to normalize the total genomic DNA amount. Absolute quantification was measured by comparing serial dilutions of a plasmid standard containing both sequences.

Identification of Clonal Expansion and Calculation of Replating Frequencies

Outgrowth was determined initially by microscope, followed by MTT assay. Prior research had demonstrated that 4× SD of all readings reproduced the microscopic scoring and was determined as the threshold value distinguished from background absorbance readings in the MTT assay. If the measured absorbance was above the threshold, then the well was scored as positive in the MTT matrix. Clonal outgrowth was independently screened by two technologists in four categories. Category 1 is a robust outgrowth with a visible pH change of the medium. Category 2 is obvious outgrowth of cells. Category 3 shows some level of proliferation and may be assigned to category 2 in case of a positive result in the MTT assay. Category 4 shows no cell growth and scores as negative in the MTT assay.

The RF was calculated from the number of wells above threshold using the L-Calc software (version 1.1) from STEMCELL Technologies according to Poisson distribution. The risk of insertional mutagenesis was correlated to the number of vector copies per cell, and RFs were normalized to the VCN.

Insertion Site Analysis

LAM-PCR[50] was performed using genomic DNA (300 ng) as a template. PCR amplicons were visualized on a 2% agarose gel. Specific bands were excised, purified, and directly sequenced.

Flow Cytometry

PBMCs and BMMNCs were collected from mice at the time of analysis. RBCs were lysed in RBC lysing buffer (Sigma-Aldrich; 8.3 g/L ammonium chloride in 0.01M Tris-HCl buffer [pH 7.5 ± 0.2]) according to the manufacturer's instructions. Cells were washed with 1× PBS and resuspended in fluorescence-activated cell sorting (FACS) buffer (PBS, 2% fetal bovine serum, 1 mmol/L ethylenediaminetetraacetic acid, and 0.1% NaN_3) on ice and stained with PE-hCD45 or PE-hCD34 or the corresponding isotype. Cells were then analyzed by flow cytometry using a FACSCalibur (BD Biosciences), and data were analyzed by CellQuestPro and FlowJo software.

Statistical Analysis

Results are expressed as mean ± SD or SEM as indicated. Differences between groups were assessed using Student's t test or ANOVA. Values of $p < 0.05$ were considered to be significantly different.

SUPPLEMENTAL INFORMATION

Supplemental Information includes three figures and four tables and can be found with this article online at http://dx.doi.org/10.1016/j.omtm.2017.05.003.

AUTHOR CONTRIBUTIONS

Conceptualization, J.A.M., A. Khan., M.L.W., R.F, and A. Keating.; Methodology, J.A.M., A. Khan., R.F., N.L.P., C.A.B., C.A.R., J.H., and B.C.A.; Investigation, J.H., B.C.A., L.L.V., N.L.P., M.B., M.R., J.W.R., M.A., M.S.N., S.D., A.S., and P.V.T.; Writing – Original Draft, J.H., D.L.B., and J.A.M.; Writing – Review & Editing, J.A.M., J.H., D.L.B., A. Khan., and M.L.W.; Resources, J.A.M, A. Khan., N.L.P., A. Keating., M.L.W., J.K., S.S., C.A.R., C.A.B., and R.F.; Supervision, J.A.M, A. Khan., D.L.B., A. Keating., M.L.W., S.S., C.A.R., C.A.B., and R.F.

CONFLICTS OF INTEREST

J.A.M. is an academic founder and shareholder in AVROBIO, Inc.

ACKNOWLEDGMENTS

This study was supported jointly by The Canadian Institutes of Health Research and the Kidney Foundation of Canada (The FACTs Project: Fabry Disease Clinical Research and Therapeutics) and University of Calgary Cumming School of Medicine and Alberta Health Services. The authors thank Yuanfeng Liu for technical support concerning the scale-up process validation.

REFERENCES

1. Brady, R.O., Gal, A.E., Bradley, R.M., Martensson, E., Warshaw, A.L., and Laster, L. (1967). Enzymatic defect in Fabry's disease. Ceramidetrihexosidase deficiency. N. Engl. J. Med. *276*, 1163–1167.
2. Desnick, R.J., Brady, R., Barranger, J., Collins, A.J., Germain, D.P., Goldman, M., Grabowski, G., Packman, S., and Wilcox, W.R. (2003). Fabry disease, an under-recognized multisystemic disorder: expert recommendations for diagnosis, management, and enzyme replacement therapy. Ann. Intern. Med. *138*, 338–346.
3. Waldek, S., Patel, M.R., Banikazemi, M., Lemay, R., and Lee, P. (2009). Life expectancy and cause of death in males and females with Fabry disease: findings from the Fabry Registry. Genet. Med. *11*, 790–796.
4. Houge, G., and Skarbøvik, A.J. (2005). [Fabry disease–a diagnostic and therapeutic challenge]. Tidsskr. Nor. Laegeforen. *125*, 1004–1006.
5. Meikle, P.J., Hopwood, J.J., Clague, A.E., and Carey, W.F. (1999). Prevalence of lysosomal storage disorders. JAMA *281*, 249–254.
6. Hwu, W.L., Chien, Y.H., Lee, N.C., Chiang, S.C., Dobrovolny, R., Huang, A.C., Yeh, H.Y., Chao, M.C., Lin, S.J., Kitagawa, T., et al. (2009). Newborn screening for Fabry disease in Taiwan reveals a high incidence of the later-onset *GLA* mutation c.936+919G>A (IVS4+919G>A). Hum. Mutat. *30*, 1397–1405.
7. Inoue, T., Hattori, K., Ihara, K., Ishii, A., Nakamura, K., and Hirose, S. (2013). Newborn screening for Fabry disease in Japan: prevalence and genotypes of Fabry disease in a pilot study. J. Hum. Genet. *58*, 548–552.
8. Mechtler, T.P., Metz, T.F., Müller, H.G., Ostermann, K., Ratschmann, R., De Jesus, V.R., Shushan, B., Di Bussolo, J.M., Herman, J.L., Herkner, K.R., and Kasper, D.C. (2012). Short-incubation mass spectrometry assay for lysosomal storage disorders in newborn and high-risk population screening. J. Chromatogr. B Analyt. Technol. Biomed. Life Sci. *908*, 9–17.
9. Scott, C.R., Elliott, S., Buroker, N., Thomas, L.I., Keutzer, J., Glass, M., Gelb, M.H., and Turecek, F. (2013). Identification of infants at risk for developing Fabry, Pompe, or mucopolysaccharidosis-I from newborn blood spots by tandem mass spectrometry. J. Pediatr. *163*, 498–503.

10. Spada, M., Pagliardini, S., Yasuda, M., Tukel, T., Thiagarajan, G., Sakuraba, H., Ponzone, A., and Desnick, R.J. (2006). High incidence of later-onset fabry disease revealed by newborn screening. Am. J. Hum. Genet. *79*, 31–40.

11. Uribe, A., and Giugliani, R. (2013). Selective screening for lysosomal storage diseases with dried blood spots collected on filter paper in 4,700 high-risk colombian subjects. JIMD Rep. *11*, 107–116.

12. Wittmann, J., Karg, E., Turi, S., Legnini, E., Wittmann, G., Giese, A.K., Lukas, J., Gölnitz, U., Klingenhäger, M., Bodamer, O., et al. (2012). Newborn screening for lysosomal storage disorders in hungary. JIMD Rep. *6*, 117–125.

13. Liao, H.C., Chiang, C.C., Niu, D.M., Wang, C.H., Kao, S.M., Tsai, F.J., Huang, Y.H., Liu, H.C., Huang, C.K., Gao, H.J., et al. (2014). Detecting multiple lysosomal storage diseases by tandem mass spectrometry–a national newborn screening program in Taiwan. Clin. Chim. Acta *431*, 80–86.

14. Germain, D.P., Hughes, D.A., Nicholls, K., Bichet, D.G., Giugliani, R., Wilcox, W.R., Feliciani, C., Shankar, S.P., Ezgu, F., Amartino, H., et al. (2016). Treatment of Fabry's Disease with the Pharmacologic Chaperone Migalastat. N. Engl. J. Med. *375*, 545–555.

15. Pacienza, N., Yoshimitsu, M., Mizue, N., Au, B.C., Wang, J.C., Fan, X., Takenaka, T., and Medin, J.A. (2012). Lentivector transduction improves outcomes over transplantation of human HSCs alone in NOD/SCID/Fabry mice. Mol. Ther. *20*, 1454–1461.

16. Scaife, M., Pacienza, N., Au, B.C., Wang, J.C., Devine, S., Scheid, E., Lee, C.J., Lopez-Perez, O., Neschadim, A., Fowler, D.H., et al. (2013). Engineered human Tmpk fused with truncated cell-surface markers: versatile cell-fate control safety cassettes. Gene Ther. *20*, 24–34.

17. Takenaka, T., Qin, G., Brady, R.O., and Medin, J.A. (1999). Circulating alpha-galactosidase A derived from transduced bone marrow cells: relevance for corrective gene transfer for Fabry disease. Hum. Gene Ther. *10*, 1931–1939.

18. Takenaka, T., Murray, G.J., Qin, G., Quirk, J.M., Ohshima, T., Qasba, P., Clark, K., Kulkarni, A.B., Brady, R.O., and Medin, J.A. (2000). Long-term enzyme correction and lipid reduction in multiple organs of primary and secondary transplanted Fabry mice receiving transduced bone marrow cells. Proc. Natl. Acad. Sci. USA *97*, 7515–7520.

19. Sugimoto, Y., Aksentijevich, I., Murray, G.J., Brady, R.O., Pastan, I., and Gottesman, M.M. (1995). Retroviral coexpression of a multidrug resistance gene (MDR1) and human alpha-galactosidase A for gene therapy of Fabry disease. Hum. Gene Ther. *6*, 905–915.

20. Medin, J.A., Tudor, M., Simovitch, R., Quirk, J.M., Jacobson, S., Murray, G.J., and Brady, R.O. (1996). Correction in trans for Fabry disease: expression, secretion and uptake of alpha-galactosidase A in patient-derived cells driven by a high-titer recombinant retroviral vector. Proc. Natl. Acad. Sci. USA *93*, 7917–7922.

21. Takiyama, N., Dunigan, J.T., Vallor, M.J., Kase, R., Sakuraba, H., and Barranger, J.A. (1999). Retrovirus-mediated transfer of human alpha-galactosidase A gene to human CD34+ hematopoietic progenitor cells. Hum. Gene Ther. *10*, 2881–2889.

22. Yoshimitsu, M., Higuchi, K., Dawood, F., Rasaiah, V.I., Ayach, B., Chen, M., Liu, P., and Medin, J.A. (2006). Correction of cardiac abnormalities in fabry mice by direct intraventricular injection of a recombinant lentiviral vector that engineers expression of alpha-galactosidase A. Circ. J. *70*, 1503–1508.

23. Jung, S.C., Han, I.P., Limaye, A., Xu, R., Gelderman, M.P., Zerfas, P., Tirumalai, K., Murray, G.J., During, M.J., Brady, R.O., and Qasba, P. (2001). Adeno-associated viral vector-mediated gene transfer results in long-term enzymatic and functional correction in multiple organs of Fabry mice. Proc. Natl. Acad. Sci. USA *98*, 2676–2681.

24. Yoshimitsu, M., Higuchi, K., Ramsubir, S., Nonaka, T., Rasaiah, V.I., Siatskas, C., Liang, S.B., Murray, G.J., Brady, R.O., and Medin, J.A. (2007). Efficient correction of Fabry mice and patient cells mediated by lentiviral transduction of hematopoietic stem/progenitor cells. Gene Ther. *14*, 256–265.

25. Kozak, M. (1987). An analysis of 5′-noncoding sequences from 699 vertebrate messenger RNAs. Nucleic Acids Res. *15*, 8125–8148.

26. Yoshimitsu, M., Sato, T., Tao, K., Walia, J.S., Rasaiah, V.I., Sleep, G.T., Murray, G.J., Poeppl, A.G., Underwood, J., West, L., et al. (2004). Bioluminescent imaging of a marking transgene and correction of Fabry mice by neonatal injection of recombinant lentiviral vectors. Proc. Natl. Acad. Sci. USA *101*, 16909–16914.

27. Ohshima, T., Murray, G.J., Swaim, W.D., Longenecker, G., Quirk, J.M., Cardarelli, C.O., Sugimoto, Y., Pastan, I., Gottesman, M.M., Brady, R.O., and Kulkarni, A.B. (1997). alpha-Galactosidase A deficient mice: a model of Fabry disease. Proc. Natl. Acad. Sci. USA *94*, 2540–2544.

28. Huang, J., Liu, Y., Au, B.C., Barber, D.L., Arruda, A., Schambach, A., Rothe, M., Minden, M.D., Paige, C.J., and Medin, J.A. (2016). Preclinical validation: LV/IL-12 transduction of patient leukemia cells for immunotherapy of AML. Mol. Ther. Methods Clin. Dev. *3*, 16074.

29. Baehner, F., Kampmann, C., Whybra, C., Miebach, E., Wiethoff, C.M., and Beck, M. (2003). Enzyme replacement therapy in heterozygous females with Fabry disease: results of a phase IIIB study. J. Inherit. Metab. Dis. *26*, 617–627.

30. Banikazemi, M., Bultas, J., Waldek, S., Wilcox, W.R., Whitley, C.B., McDonald, M., Finkel, R., Packman, S., Bichet, D.G., Warnock, D.G., and Desnick, R.J.; Fabry Disease Clinical Trial Study Group (2007). Agalsidase-beta therapy for advanced Fabry disease: a randomized trial. Ann. Intern. Med. *146*, 77–86.

31. Eng, C.M., Guffon, N., Wilcox, W.R., Germain, D.P., Lee, P., Waldek, S., Caplan, L., Linthorst, G.E., and Desnick, R.J.; International Collaborative Fabry Disease Study Group (2001). Safety and efficacy of recombinant human alpha-galactosidase A replacement therapy in Fabry's disease. N. Engl. J. Med. *345*, 9–16.

32. Germain, D.P., Waldek, S., Banikazemi, M., Bushinsky, D.A., Charrow, J., Desnick, R.J., Lee, P., Loew, T., Vedder, A.C., Abichandani, R., et al. (2007). Sustained, long-term renal stabilization after 54 months of agalsidase beta therapy in patients with Fabry disease. J. Am. Soc. Nephrol. *18*, 1547–1557.

33. Hughes, D.A., Elliott, P.M., Shah, J., Zuckerman, J., Coghlan, G., Brookes, J., and Mehta, A.B. (2008). Effects of enzyme replacement therapy on the cardiomyopathy of Anderson-Fabry disease: a randomised, double-blind, placebo-controlled clinical trial of agalsidase alfa. Heart *94*, 153–158.

34. Schiffmann, R., Kopp, J.B., Austin, H.A., 3rd, Sabnis, S., Moore, D.F., Weibel, T., Balow, J.E., and Brady, R.O. (2001). Enzyme replacement therapy in Fabry disease: a randomized controlled trial. JAMA *285*, 2743–2749.

35. Schwarting, A., Dehout, F., Feriozzi, S., Beck, M., Mehta, A., and Sunder-Plassmann, G.; European FOS Investigators (2006). Enzyme replacement therapy and renal function in 201 patients with Fabry disease. Clin. Nephrol. *66*, 77–84.

36. Thurberg, B.L., Rennke, H., Colvin, R.B., Dikman, S., Gordon, R.E., Collins, A.B., Desnick, R.J., and O'Callaghan, M. (2002). Globotriaosylceramide accumulation in the Fabry kidney is cleared from multiple cell types after enzyme replacement therapy. Kidney Int. *62*, 1933–1946.

37. Wilcox, W.R., Banikazemi, M., Guffon, N., Waldek, S., Lee, P., Linthorst, G.E., Desnick, R.J., and Germain, D.P.; International Fabry Disease Study Group (2004). Long-term safety and efficacy of enzyme replacement therapy for Fabry disease. Am. J. Hum. Genet. *75*, 65–74.

38. Biffi, A., Montini, E., Lorioli, L., Cesani, M., Fumagalli, F., Plati, T., Baldoli, C., Martino, S., Calabria, A., Canale, S., et al. (2013). Lentiviral hematopoietic stem cell gene therapy benefits metachromatic leukodystrophy. Science *341*, 1233158.

39. Ungari, S., Montepeloso, A., Morena, F., Cocchiarella, F., Recchia, A., Martino, S., Gentner, B., Naldini, L., and Biffi, A. (2015). Design of a regulated lentiviral vector for hematopoietic stem cell gene therapy of globoid cell leukodystrophy. Mol. Ther. Methods Clin. Dev. *2*, 15038.

40. Jiang, X., Hanna, Z., Kaouass, M., Girard, L., and Jolicoeur, P. (2002). Ahi-1, a novel gene encoding a modular protein with WD40-repeat and SH3 domains, is targeted by the Ahi-1 and Mis-2 provirus integrations. J. Virol. *76*, 9046–9059.

41. Jiang, X., Zhao, Y., Chan, W.Y., Vercauteren, S., Pang, E., Kennedy, S., Nicolini, F., Eaves, A., and Eaves, C. (2004). Deregulated expression in Ph+ human leukemias of AHI-1, a gene activated by insertional mutagenesis in mouse models of leukemia. Blood *103*, 3897–3904.

42. Dixon-Salazar, T., Silhavy, J.L., Marsh, S.E., Louie, C.M., Scott, L.C., Gururaj, A., Al-Gazali, L., Al-Tawari, A.A., Kayserili, H., Sztriha, L., and Gleeson, J.G. (2004). Mutations in the AHI1 gene, encoding jouberin, cause Joubert syndrome with cortical polymicrogyria. Am. J. Hum. Genet. *75*, 979–987.

43. Ferland, R.J., Eyaid, W., Collura, R.V., Tully, L.D., Hill, R.S., Al-Nouri, D., Al-Rumayyan, A., Topcu, M., Gascon, G., Bodell, A., et al. (2004). Abnormal cerebellar development and axonal decussation due to mutations in AHI1 in Joubert syndrome. Nat. Genet. *36*, 1008–1013.

44. Fischer, A., Schumacher, N., Maier, M., Sendtner, M., and Gessler, M. (2004). The Notch target genes Hey1 and Hey2 are required for embryonic vascular development. Genes Dev. *18*, 901–911.

45. Wang, L., Motoi, T., Khanin, R., Olshen, A., Mertens, F., Bridge, J., Dal Cin, P., Antonescu, C.R., Singer, S., Hameed, M., et al. (2012). Identification of a novel, recurrent HEY1-NCOA2 fusion in mesenchymal chondrosarcoma based on a genome-wide screen of exon-level expression data. Genes Chromosomes Cancer *51*, 127–139.

46. Aiuti, A., Biasco, L., Scaramuzza, S., Ferrua, F., Cicalese, M.P., Baricordi, C., Dionisio, F., Calabria, A., Giannelli, S., Castiello, M.C., et al. (2013). Lentiviral hematopoietic stem cell gene therapy in patients with Wiskott-Aldrich syndrome. Science *341*, 1233151.

47. Mitchell, R.S., Beitzel, B.F., Schroder, A.R., Shinn, P., Chen, H., Berry, C.C., Ecker, J.R., and Bushman, F.D. (2004). Retroviral DNA integration: ASLV, HIV, and MLV show distinct target site preferences. PLoS Biol. *2*, E234.

48. Wang, J.C., Felizardo, T.C., Au, B.C., Fowler, D.H., Dekaban, G.A., and Medin, J.A. (2013). Engineering lentiviral vectors for modulation of dendritic cell apoptotic pathways. Virol. J. *10*, 240.

49. Provençal, P., Boutin, M., Dworski, S., Au, B., Medin, J.A., and Auray-Blais, C. (2016). Relative distribution of Gb3 isoforms/analogs in NOD/SCID/Fabry mice tissues determined by tandem mass spectrometry. Bioanalysis *8*, 1793–1807.

50. Schmidt, M., Schwarzwaelder, K., Bartholomae, C., Zaoui, K., Ball, C., Pilz, I., Braun, S., Glimm, H., and von Kalle, C. (2007). High-resolution insertion-site analysis by linear amplification-mediated PCR (LAM-PCR). Nat. Methods *4*, 1051–1057.